OXFORD UNIVERSITY PRESS | Brain

Brain catecholamine depletion and motor impairment in a Th knock-in mouse with type B tyrosine hydroxylase deficiency

Journal:	*Brain*
Manuscript ID:	BRAIN-2015-00246.R2
Manuscript Type:	Original Article
Date Submitted by the Author:	n/a
Complete List of Authors:	Korner, Germaine; University of Zurich, Noain, Daniela; University of Zurich, Ying, Ming; University of Bergen, Hole, Magnus; University of Bergen, Flydal, Marte; University of Bergen, Scherer, Tanja; University of Zurich, Allegri, Gabriella; University of Zurich, Rassi, Anahita; University of Zurich, Fingerhut, Ralph; University of Zurich, Becu-Villalobos, Damasia; Institute of Biology and Experimental Medicine, Pillai, Samyuktha; University of Zurich, Wuuest, Stephan; University of Zurich, Konrad, Daniel; University of Zurich, Lauber-Biason, Anna; University of Fribourg, Baumann, Christian; University Hospital Zurich, Neurology Department Bindoff, Laurence; Haukeland University Hospital, Department of Neurology; University of Bergen, Department of Clinical Medicine Martinez, A; University of Bergen, Department of Biomedicine Thony, Beat; University of Zurich, Department of Pediatrics
Subject category:	Movement disorders
To search keyword list, use whole or part words followed by an *:	Genetics: neuropathy < GENETICS, Metabolic disease < GENETICS, Dystonia < MOVEMENT DISORDERS, Movement disorders: other < MOVEMENT DISORDERS, Cerebrospinal fluid < SYSTEMS/DEVELOPMENT/PHYSIOLOGY

Brain catecholamine depletion and motor impairment in a *Th* knock-in mouse with type B tyrosine hydroxylase deficiency

Germaine Korner,[1,2,3,¶] Daniela Noain,[4,¶] Ming Ying,[5] Magnus Hole,[5] Marte I. Flydal,[5] Tanja Scherer,[1,3] Gabriella Allegri,[1,3] Anahita Rassi,[6] Ralph Fingerhut,[7,3] Damasia Becu-Villalobos,[8] Samyuktha Pillai,[9] Stephan Wueest,[3,10] Daniel Konrad,[3,10] Anna Lauber-Biason,[11] Christian R. Baumann,[2,4] Laurence A. Bindoff,[12,13] Aurora Martinez[5,*] and Beat Thöny[1,2,3,*]

(1) Division of Metabolism, Department of Pediatrics, University of Zürich, Zürich, Switzerland
(2) Affiliated with the Neuroscience Center Zurich (ZNZ), Zürich, Switzerland
(3) Affiliated with the Children's Research Centre (CRC), Zürich, Switzerland
(4) Department of Neurology, University Hospital of Zurich, Zürich, Switzerland
(5) Department of Biomedicine, University of Bergen, Bergen, Norway
(6) Division of Clinical Chemistry and Biochemistry, Department of Pediatrics, University of Zürich, Zürich, Switzerland
(7) Swiss Newborn Screening Laboratory, University Children's Hospital, Zurich, Switzerland
(8) Institute of Biology and Experimental Medicine, Buenos Aires, Argentina
(9) Institute of Physiology, University of Zurich, Zürich, Switzerland
(10) Division of Endocrinology, Department of Pediatrics, University of Zurich, Switzerland
(11) Department of Medicine, University of Fribourg, Fribourg, Switzerland
(12) Department of Clinical Medicine (K1), University of Bergen, Norway
(13) Department of Neurology, Haukeland University Hospital, Bergen, Norway

*Shared correspondence:
Dr. Aurora Martinez, Department of Biomedicine, University of Bergen, Jonas Lies vei 91, 5009 Bergen, Norway, Tel: +47 55586427, aurora.martinez@biomed.uib.no
Dr. Beat Thöny, Division of Metabolism, Department of Pediatrics, University of Zurich, Steinwiesstrasse 75, CH-8032 Zürich, Switzerland, Tel +41 44 2667622; beat.thony@kispi.uzh.ch

¶These authors contributed equally to this work

Running title Molecular mechanism for severe TH deficiency

Key words: infantile parkinsonism, dopamine deficiency, catecholamine deficiency, misfolding, mislocalization

Abbreviations: BH_4, (6*R*)-L-*erythro*-5,6,7,8-tetrahydrobiopterin; DA, dopamine; DRD, Dopa-responsive dystonia; 5-HIAA, 5-hydroxyindolacetic acid; 5-HTP, 5-hydroxytryptophan; HVA, homovanillic acid; IGF-1, insulin-like growth factor 1; L-Dopa, L-dihydroxyphenylalanine; L-Tyr, L-tyrosine; MHPG, 3-methoxy-4-hydroxyphenylethylene glycol; TH, tyrosine hydroxylase; THD, tyrosine hydroxylase deficiency; tT4, total thyroid hormone thyroxine.

Abstract

Tyrosine hydroxylase catalyzes the hydroxylation of L-tyrosine to L-Dopa, the rate-limiting step in the synthesis of catecholamines. Mutations in the *TH* gene encoding tyrosine hydroxylase are associated with the autosomal recessive disorder tyrosine hydroxylase deficiency, which manifests phenotypes varying from infantile parkinsonism and Dopa-responsive dystonia, also termed type A, to complex encephalopathy with perinatal onset, termed type B. We generated homozygous *Th*-knock-in mice with the mutation *Th*-p.R203H, equivalent to the most recurrent human mutation associated with type B tyrosine hydroxylase deficiency (*TH*-p.R233H), often unresponsive to L-Dopa treatment. The *Th*-knock-in mice showed normal survival and food intake, but hypotension, hypokinesia, reduced motor coordination, wide-based gate and catalepsy. This phenotype was associated to a gradual loss of central catecholamines and the serious manifestations of motor impairment presented diurnal fluctuation but did not improve with standard L-Dopa treatment. The mutant tyrosine hydroxylase enzyme was unstable and exhibited deficient stabilization by catecholamines, leading to decline of brain tyrosine hydroxylase-immunoreactivity in the *Th* knock-in mice. In fact the *substantia nigra* presented an almost normal level of mutant tyrosine hydroxylase protein but distinct absence of the enzyme was observed in the striatum, indicating a mutation-associated mislocalization of tyrosine hydroxylase in the nigrostriatal pathway. This hypomorphic mouse model thus provides understanding on pathomechanisms in type B tyrosine hydroxylase deficiency and a platform for the evaluation of novel therapeutics for movement disorders with loss of dopaminergic input to the striatum.

Introduction

Tyrosine hydroxylase (TH; EC 1.14.16.2) is a homo-tetrameric enzyme that catalyzes the conversion of L-tyrosine (L-Tyr) to L-dihydroxyphenylalanine (L-Dopa) by using molecular oxygen as additional substrate and the cofactor (6*R*)-L-*erythro*-5,6,7,8-tetrahydrobiopterin (BH_4) (Nagatsu *et al.*, 1964, Roberts and Fitzpatrick, 2013). This hydroxylation is the rate limiting step in the synthesis of the catecholamine neurotransmitters dopamine (DA), norepinephrine and epinephrine (Nagatsu *et al.*, 1964). DA is distinctively involved in motor control, but also in cognition, memory and reward, and, as a precursor of norepinephrine and epinephrine, indirectly regulates attention and helps to maintain normal blood pressure and blood sugar (Eisenhofer *et al.*, 2004). In the central nervous system (CNS), TH is mainly expressed in dopaminergic neurons of the *substantia nigra* that projects mostly to the striatum and has a central role in motor control, and in the ventral *tegmental area* (VTA) that mainly projects to the *nucleus accumbens* and *the prefrontal cortex* and regulates motivation and reward. TH is also expressed in noradrenergic neurons of the *locus coeruleus* and *lateral tegmental* system (Zigmond *et al.*, 1989, Bjorklund and Dunnett, 2007). Outside the CNS, TH expression is found in the *adrenal medulla*, the sympathetic neurons, and in non-neuronal (renal, intestine, pancreatic and lymphoid) tissues. The single human *TH* gene undergoes alternative mRNA splicing generating four main isoforms (hTH1-hTH4), with variations in the length of the N-terminal, where hTH4 corresponds to the longest, full-length isoform and hTH1 to the shortest and most abundant one, equivalent to rodent TH (Nagatsu, 1995). TH activity is tightly controlled by regulatory mechanisms at the transcriptional, translational and posttranslational levels (Kumer and Vrana, 1996, Tank *et al.*, 2008). The latter includes phosphorylation at several Ser/Thr residues at the N-terminal tail (Daubner *et al.*, 2011). Notably, phosphorylation at Ser40 by cAMP dependent protein kinase A activates TH by releasing the feedback inhibition of catecholamines and decreasing the K_m for the cofactor BH_4 (Nagatsu *et al.*, 1964). Binding of the catecholamine end-products inactivates and stabilizes TH both *in vitro* (Okuno and Fujisawa, 1991, Martinez *et al.*, 1996) and *in vivo* (Sumi-Ichinose *et al.*, 2001). Another short-term regulatory mechanism of TH of important biological significance is substrate inhibition, that allows steady synthesis of DA despite fluctuations in blood L-tyrosine (Reed *et al.*, 2010).

Mutations in the *TH* gene (OMIM *191290) cause TH deficiency (THD; OMIM #605407), which is a rare disorder that comprises a broad phenotypic variation including infantile parkinsonism and Dopa-responsive dystonia (DRD). THD manifestations range from a mild progressive limb dystonia, postural tremor and hypokinetic rigid syndrome that is responsive to Dopa (termed type A) to a progressive and complex neonatal or early-infancy onset encephalopathy with Dopa-unresponsive parkinsonism (termed type B) (Willemsen *et al.*, 2010). A certain genotype-phenotype correlation between the clinical subtype and the genotype of the THD patients through the *in vitro* TH activity of the mutant variants has

recently been reported (Fossbakk *et al.*, 2014). Nevertheless, an accurate clinical diagnosis of THD must be based on central catecholamine deficiency reflected by normal 5-hydroxyindolacetic acid (5-HIAA) but low homovanillic acid (HVA), low 3-methoxy-4-hydroxyphenylethylene glycol (MHPG) and low HVA:5-HIAA ratio in CSF from lumbar puncture (Willemsen *et al.*, 2010), and by mutation analysis of the *TH* gene (Haavik *et al.*, 2008, Kurian *et al.*, 2011). Peripheral (urinary) concentration of catecholamines, HVA and MHPG are non-informative most probably due to DA production by residual TH and tyrosinase activity in non-neuronal tissues (for a discussion see (Willemsen *et al.*, 2010)). Elevated serum prolactin may, however, be used as a peripheral biomarker reflecting central neurotransmitter status (Aitkenhead and Heales, 2013). The release of this hormone from the pituitary gland is under control of hypothalamic DA, which is the primary physiological inhibitor of prolactin secretion (Ben-Jonathan, 1985). Furthermore, galactorrhoea has been observed in some severely affected hyperprolactinemic THD patients (Yeung *et al.*, 2006). To date, approximately 70 THD patients have been reported (www.biopku.org/pnddb) (Willemsen *et al.*, 2010, Fossbakk *et al.*, 2014); the most recurrent *TH* mutation, accounting for ~30% of all mutant alleles, is c.698G>A/p.Arg233His in exon 6; NM_1999292.2 (corresponding to c.605G>A/p.Arg202His in hTH1). While as a homozygous or compound heterozygous allele this mutation can be associated with both type A or type B THD (Haavik *et al.*, 2008, Willemsen *et al.*, 2010), about half of the patients with type B THD are homozygous for variant p.R233H (Willemsen *et al.*, 2010).

Parkinsonian syndromes, dystonias, and related movement disorders showing a reduction in the levels of TH activity and DA levels are closely associated to THD (Kurian *et al.*, 2011, Garcia-Cazorla and Duarte, 2014). Although THD is not accompanied by neurodegeneration, it shares several traits with Parkinson's disease where the motor features actually reflect the loss of *striatal* DA due to degeneration of dopaminergic neurons in the midbrain (Obeso *et al.*, 2010). Transgenic mouse models aiming to mimic TH deficiency by inactivating the *Th* gene have been generated in the past (Kobayashi *et al.*, 1995, Zhou *et al.*, 1995, Szczypka *et al.*, 1999). The complete *Th*-knock-out was non-viable, and none of the rescue mutants fully reproduced the clinical and pathological features of THD. They did however provide valuable insights into the importance of DA and the other catecholamines for mouse fetal development (Kobayashi *et al.*, 1995, Zhou *et al.*, 1995) and the functional interdependence of the adrenomedullary and adrenocortical systems (Bornstein *et al.*, 2000).

In order to provide novel insights into catecholamine function and study the pathophysiological mechanisms responsible for the severe (type B) THD phenotype, we generated a constitutive *Th*-knock-in mouse with the p.Arg203His mutation, equivalent to the human *TH*-p.R233H *(*h*TH*1-p.R202H). This mouse, here termed *Th*-ki, was viable and presented with motor dysfunction due to a reduced TH activity and gradual loss of

catecholamine metabolites, including DA. Measurements in brain extracts, immunohistochemical analyses and kinetic and molecular studies of wild-type (wt) and mutant human and mouse enzymes showed the instability of the mutant TH. Importantly, the mutant enzymes could not be stabilized by DA, highlighting the importance of a functional regulatory feedback inhibition by catecholamines to maintain TH levels and proper localization. Furthermore, the *Th*-ki mouse displays the salient clinical features of human type B THD phenotype including biochemical markers, impaired motor function, diurnal fluctuation of symptoms and non-responsiveness to L-Dopa treatment, and thus represents an ideal model for pathomechanistic studies and for investigations of novel therapeutic approaches, such as pharmacological chaperones and treatment strategies based on circadian regulation of TH activity and/or restorative properties of sleep.

Materials and Methods, and Mouse Husbandry

Generation of the *Th*-ki mouse allele

A C57BL/6 mouse carrying a constitutive knock-in of the point mutation p.Arg203His in the *Th* gene was custom generated by TaconicArtemis (Cologne, Germany; NCBI gene ID 21823, transcript variant *Th*-1 NM_0093771.1; Ensembl gene ID ENSMUSG00000000214). Details on the targeting vector for electroporation, homologous recombination and selection in mouse embryonic stem cells (Art B6/3.6 background C57BL/6 NTac) are given in Supplementary Figures 1A-C. Validation of correct and single targeting was done by Southern blot and PCR analyses (details can be supplied upon request). For elimination of the *NeoR* cassette, mice were crossed with a FLP-deleter strain (C57BL/6-*Tg*(CAG-*Flpe*)1 Arte) for random integration of the CAGGS-FLPe transgene, and subsequently mice were crossed to homozygosity.

Genotyping of *Th*-ki mice

One primer set was used for testing for the presence of an additional 85 bp FRT sequence by fragment size analysis (primers "For" 4601_33: 5'-GAGCTCCCAGAATTGACAGC-3'; "Rev" 4601_34: 5'-GATCACACTCCACCATATCAAGG-3') and another set for the presence of the R203H mutation via Sanger sequencing (primers 4602_35: 5'-TGTCAGAGTTGGATAAGTGTCACC-3' and 4602_36: 5'-TGACAGCTAACCAGTCACCTCC-3'; see also Supplementary Figures 1B,C). Standard PCR conditions were used for DNA amplification.

Mouse husbandry and treatment studies

Animal experiments were performed in accordance with the guidelines and policies of the Veterinary Office of the State of Zurich and Swiss law on animal protection, the Swiss Federal Act on Animal Protection (1978), and the Swiss Animal Protection Ordinance (1981). Animal studies received approval from by the Cantonal Veterinary Office, Zurich, and the Cantonal Committee for Animal Experiments, Zurich, Switzerland. All mice are generated by back-crossing with C57BL/6J from the Jackson Laboratory (i.e. C57BL/6J, α-synuclein positive), and for control, we used exclusively the wild-type littermates. Mice were maintained in humidity and temperature (21-23 °C) controlled under a 12 h dark-light cycle. For treatment studies, 6 tablets containing L-Dopa (levodopa 100 mg) and the decarboxylase inhibitor carbidopa (25 mg) were purchased (Sinemet) and diluted in 20 ml of ddH_20. For validation, the final concentration of L-Dopa was determined by HPLC (Blau *et al.*, 1999). Newborn homozygous *Th*-ki and wt control mice were fed for the *chronic* experiments daily *per os* with a solution containing 10 mg levodopa plus 2.5 mg carbidopa per kg of body weight and per day for a time period of up to 3 weeks of age. Elevation of brain 3-OMD and HVA control supported that mice received adequate doses of L-Dopa (see Fig. 8). Treated mice were tested 24 h after the last administration for motor behavior, and upon sacrifice

tissue was collected for biochemical analyses. Mock control, independent groups of *Th*-ki and wt mice, sex and aged-matched were given ddH_2O in parallel. For the *acute* L-Dopa treatment experiment, a group of *Th*-ki plus wt control mice were first mock fed and tested for motor function (rotarod and bar test; see below). Following a resting phase of 2-3 h, all mice were loaded *per os* with a single bolus of a solution containing 10 mg levodopa plus 2.5 mg carbidopa per kg of body weight, before re-testing these mice for motor coordination within 20-45 min after the L-Dopa loading.

Metabolic cage analysis

Locomotion, food and water intake, O_2 consumption and CO_2 production were determined for single housed mice (females at the age of 9 months) during a 24-h period in metabolic cages in an open-circuit indirect calorimetry system as previously described (Wueest *et al.*, 2014) (PhenoMaster, TSE Systems, Bad Homburg, Germany). After being adapted to single caging, mice were placed in cages closed with air-tight lids. Water bottles and food cups were placed on scales to measure water and food intake continuously. The measurements were saved on a computer in 20 min intervals and were used to calculate cumulative food and water intake. Activity data were measured using an infrared light-beam. To measure energy expenditure (EE) and respiratory exchange ratio (RER), ambient air was pumped through the cage via a flow controller. Air entering and leaving each cage was monitored for its O_2 and CO_2 concentration. The cages were connected to two analyzers measuring O_2/CO_2 concentration of each cage for a period of 2 min in 20 min intervals. EE and RER were calculated using the manufacturer's software based on the following equation: EE (kcal/h) = $(3.941 \times VO_2 + 1.106 \times VCO_2)/1000$; $RER = VCO_2/VO_2$.

Behavioral motor testing

Experiments were carried out during the light-phase, between 10 am and 5 pm, and always at the same time of the day within the same group of animals. Experimental batches were acclimated to the test room for at least 1-2 days before testing.

Open field test (Bello *et al.*, 2011): Plexiglas activity boxes monitored by a video tracking system (Ethovision, Noldus) were used to assess total horizontal activity and mean velocity of locomotion. Animals were placed in a neutral position of the acrylic boxes (40 x 40 x 46 cm) and let to explore freely and undisturbed for 30 min. Boxes were carefully cleaned between tests to minimize odor cues in the arena.

Bar test (Noain *et al.*, 2013): Spontaneous catalepsy was determined in *Th*-wt and *Th*-ki mice using the horizontal bar test in which the time of immobility (defined as immobile trunk and limbs) was assessed as described previously. Briefly, to discard the possibility of confounding freezing behavior induced by fear/stress with catalepsy, all mice were habituated to the experimental context by 2 min free exploration over the working bench and experimental setup. Following, mice were restrained by the tail, their front paws placed over the 5-cm

elevated bar (1-cm diameter, plexiglas) and the back limbs set over the working bench. Immediately after, the timer was started. A trail was considered valid when the animal remained grabbing the bar with the front paws until the timer was running (~2 sec). Usually, 2-4 trials were invalid for each mouse at the beginning of the testing session. The highest immobility score out of five valid trials was considered for the analysis of both wt and ki subjects. The cut-off of the experiment was set at 180 sec.

.

Rotarod test (Avale *et al.*, 2004): Wt and *Th*-ki mice were individually placed in a neutral position on the immobile rotarod treadmill (UgoBasile, Milan, IT, USA). Immediately, the speed was increased to 16 revolutions per min (rpm) and each mouse was given a 10 min training session. During the training session mice were repositioned on the rod after each fall. Mice were tested 3 h later for 3 min at a fixed velocity of 16 rpm, and the latency to the first fall was recorded for each subject.

Gait analysis (de Medinaceli *et al.*, 1982, Kunkel-Bagden *et al.*, 1993, Suresh Babu *et al.*, 2012): Both hind and fore paws of mice were inked with non-toxic blue and red ink, respectively. Animals were immediately placed at one end of a 30 cm acrylic alley, whose floor was covered in white absorbent paper, and encouraged to walk to the opposite end. The paper was then removed and labeled with the animal ID number for further analysis. The stride length and width were manually measured and normalized to body weight ("size") of each mouse to obtain short-step and wide-based gait indexes, respectively.

Preparation of whole brain lysates from mice

Immediately after sacrifice, whole brains were resected and shock frozen in liquid nitrogen. Frozen brains were grinded to powder under liquid nitrogen; thereafter, all procedures were carried out at 4°C. Powdered brains were "dissolved" in 1 ml of homogenization buffer containing 50 mM Tris-HCl, pH 7.5, 100 mM KCl, 1 mM dithiothreitol (DTT), 0.2 mM PMSF (stock 10 mg/ml in isopropanol), 1 µM leupeptin (stock 5 mg/ml in H_2O) and 1 µM pepstatin (stock 1 mg/ml in methanol). A TissueLyser II (Qiagen; cat. no. 85300) was used for preparation of lysate following the manufacturer protocol.

Gene (mRNA) expression studies

Total RNA was extracted from powdered mouse brains by the QIAmp RNA Blood Mini Kit (Ref. 52304; Hombrechtikon, Switzerland) and cDNA was produced by the Promega reverse transcription system (Ref. nr. A3500; Dübendorf, Switzerland). Mouse *Th*, *Tph*1/2 and *Igf*1-mRNA expression levels were performed using the commercially available ABI assays (Mm.00447546 for *Th* -mRNA; NCBI RefSeq NM_009377.1; Mm00493798_m1 for *Tph*1-mRNA, NCBI RefSeq NM_001136084.1; NM 009414.2; Mm00557717_m1 for *Tph*2-mRNA, NCBI RefSeq NM_173391.2; Mm00439560_m1 for *Igf*1-mRNA, NCBI RefSeq NM_001111274.1). The murine glyceraldehyde-3-phosphate dehydrogenase (*Gapdh*) mRNA

(ABI assay ID: Mm99999915_g1; NCBI RefSeq NM_008084.2) was used to normalize the relative *Th* and *Tph*1/2 mRNA levels. Values were calculated as described (Livak and Schmittgen, 2001).

Determination of protein, neopterin, biopterin and monoamine neurotransmitter metabolites

Protein concentration (in g/L) was determined by using the M-TP Mikroprotein kit from Beckman Coulter Synchron LX-System (Beckman Coulter Inc, Brea, CA; kit-no. 445860). Biopterin, neopterin and monoamine neurotransmitter metabolites were determined in brain tissue following published protocols (Blau *et al.*, 1999, Elzaouk *et al.*, 2003).

Total thyroxine (tT4), thyroid stimulating hormone (TSH)-and prolactin

Serum IGF-1 was determined by radioimmunoassay (RIA) using a rat IGF-1 RIA kit (DSL-2900, Bühlmann Laboratories AG, Switzerland) (Elzaouk *et al.*, 2003), total thyroxine (tT4) from whole blood dried on filter paper was measured with the "GSP^{TM} Neonatal Thyroxine kit" from PerkinElmer (Life and Analytical Sciences, Turku, Finland), serum prolactin was quantified using an ELISA kit for mouse and rat (GenWay Biotech, Inc., San Diego, CA), and glucose was measured according to standard methods on a routine Clinical Chemistry unit on a Beckman Coulter UniCel® DxC 600 (Nyon, Switzerland) following to manufacturer's instructions.

Measuring blood pressure in mice

A non-invasive computerized tail-cuff system for measuring systolic blood pressure in mice was applied as described (Krege *et al.*, 1995).

Tissue Preparation and immunohistochemistry

Adult mice at the age of 6-7 months were anesthetized with sodium pentobarbital and, after exsanguination, transcardially perfused with 4% paraformaldehyde in phosphate buffered saline (PBS, pH 7.4). Brains were immediately removed, post fixed, cryoprotected in sucrose ladder and stored at -80 ºC until further use. For free-floating immunohistochemistry, brains were cryostat sectioned in 40 µm slices, incubated for 1 h in 1% H_2O_2 and then washed. A rabbit polyclonal anti-TH antiserum was used (1:1,000; Millipore, AB152) for specific immunostainings of TH cells. Sections were incubated with primary antibody over night at 4°C together with 2% normal goat serum. After washing, sections were incubated for 2 h at room temperature with a solution containing biotinylated goat anti-rabbit IgG (1:400, VectorLaboratories, Burlingame, CA). After washing, sections were incubated with for 1 h at room temperature with avidin/biotin complex (1:200, ABC Vectastain Elite Kit, Vector) and washed twice. Finally, sections were exposed to a solution of 0.025% diaminobenzidine,

0.05% H_2O_2 in TBS buffer and monitored for color development under microscope (for a reference see also (Gelman et al., 2003)).

Congo red staining was performed over *Th*-wt and *Th*-ki brain tissue to determine the presence of amyloid deposits indicative of a neurodegenerative process (Bohnen and Jahn, 2013; Catafau and Bullich, 2015). Briefly, we mounted 40 µm cryostat sections and dried them over night. A 5 min wash in deionized water was followed by 20 min in alkaline sodium chloride solution and 20 min in Alkaline Congo red solution (Sigma-Aldrich, Cat# HT60). Then, we dehydrated the stained tissue in absolute ethanol and xylen, and finally mounted them for bright field microscopy. We counted TH positive cell bodies in the midbrain using a semi-quantitative method. Briefly, SNpc/VTA sections from 2 *Th*-wt and 2 *Th*-ki were randomly selected from a pull of stained tissue. Similar anatomical levels were included from each genotype, to avoid misrepresentation. All positive TH cell bodies were counted in 1 hemi-section from each animal. The results are expressed as % of positive TH cells in respect to wt controls ± SEM.

Additional methodological information on "*Analytical methods for in vitro and in vivo characterization of wt and mutant enzuymes"* can be found under "*Supplementary Methods*"

Results

Th-ki mice display moderate growth retardation and hypotension

A constitutive knock-in containing the *Th*-p.Arg203His was generated by homologous recombination in the C57BL/6 background and bred to homozygosity (see Supplementary Figure S1, Table S1, and Methods for details). The *Th*-ki litter size was normal with an expected Mendelian ratio and an apparently normal phenotype initially. After weaning, however, *Th*-ki mice exhibited moderate and continuous growth retardation with 25-34% less body weight compared to their wt or heterozygous littermates (Figure 1A and B). That this was not due to feeding abnormalities was confirmed quantitatively by metabolic cage analyses showing normal food intake and respiratory exchange ratio. Locomotor activity and energy expenditure were, however, reduced (see Supplementary Figure S2). Follow up examinations of mutant mice revealed no constipation, and a quantitative analysis of the fat and total energy contents in feces also revealed no differences between wt and *Th*-ki, indicating that mutant mice had normal absorption and digestion (data not shown). *Th*-ki was normoglycemic and *Igf1* gene expression was normal (mRNA of whole brain extracts; not shown) as were IGF-1 serum levels in adult mice at the age of 12 weeks (Supplementary Figure S3C). We noticed however that *Igf1*-mRNA was significantly elevated in whole brain extracts from *Th*-ki mice at the age of 3 weeks (not shown), implying that the IGF system might be involved in brain growth as it has been suggested by others (Delafontaine *et al.*, 2004). We further detected elevation of the total thyroid hormone thyroxine (tT4) (Supplementary Figure S3A) and hypotension (Supplementary Figure S3B) while serum TSH was not different between mutant and control mice (not shown). Both low bodyweight and reduced blood pressure are found in patients with type B THD (Grattan-Smith *et al.*, 2002, Willemsen *et al.*, 2010) and in mice with norepinephrine and epinephrine deficiency (Swoap *et al.*, 2004), while we found normal levels of catecholamines in adrenals and heart of adult *Th*-ki mice (data not shown) which indicated central regulation for reduced bodyweight and hypotension. Normal catecholamine content in peripheral tissues was also reported for heterozygous *Th*-knock-out mice that present a significant reduction of TH (Kobayashi *et al.*, 1995).

Gradual loss of brain catecholamines in *Th*-ki mice

Whole brain catecholamine and serotonin metabolites were measured in newborn (day 1), juvenile (3 weeks) and adult mice (12 weeks and one year). The values of brain dopamine and other catecholamines and their metabolites obtained for adult wt-mice were in a similar range to those obtained in previous studies (Thöny *et al.*, 2008, Calvo *et al.*, 2010). HVA, the major biomarker in CSF for TH deficiency in patients, was low in *Th*-ki mice at all ages, whereas L-Dopa, DA, norepinephrine and MHPG were initially normal, but fell continuously thereafter in mutant mice (Figure 2A-D). This decrease appears specific for the catecholamines and their metabolites, as serotonin, which is typically not compromised in THD, remained unchanged

both with respect to age and when compared with the values in wt-mice, and only at an advanced age, when mutant mice exhibited a striking loss of catecholamines, was a reduction of the serotonin precursor 5-hydroxytryptophan (5-HTP) observed (Figure 2D). Biopterin (and neopterin) content remained unchanged at all ages (Figure 2 and Supplementary Figure S4), as was also the case for 5-hydroxyindoleacetic acid (5-HIAA), thus leading to a reduced HVA:5-HIAA ratio in *Th*-ki mice compared to wt at all ages (see supplementary Table S2), similar as it is found in the CSF of THD patients (Willemsen *et al.*, 2010). Furthermore, we measured a consistent elevation of serum prolactin levels in adult mutant mice reflecting central DA deficiency (Supplementary Figure S3D) that caused reduced fertility of *Th*-ki females (not shown), although galactorrhoea was not observed.

Early motor dysfunction and diurnal fluctuation of the motor deficits in *Th*-ki mice

A moderate reduction of motor activity was observed in mutant mice during metabolic cage analyses (Figure S2C). In order to explore the nature of this motor dysfunction, we performed a series of behavioral tests assessing spontaneous catalepsy, motor coordination, amount and velocity of spontaneous locomotion, and gait characteristics at different ages. Motor function was tested in juvenile (3 weeks old), young adult (11 weeks old) and one year old mutant male mice plus sex and age-matched wt controls (Figures 3A to F). In the bar test, *Th*-ki mice showed increased time of immobility compared to controls, indicating spontaneous catalepsy, a sign of rigidity and inability to initiate movements. In addition, when placed at the bar, *Th*-ki mice of all ages, but particularly older adults, presented an abnormal body posture and muscle twitching, suggesting the presence of a dystonic component, while we did not observe clasping of the hindlimbs by the vertical tail suspension assay as a common test for a dystonic phenotype in mice (Sato *et al.*, 2008). *Th*-ki male mice challenged in the rotarod test showed a significantly reduced latency to fall, indicating impaired motor coordination. In the open field test, *Th*-ki mice showed significantly reduced levels of horizontal activity (amount and velocity of spontaneous locomotion), indicating a hypokinetic and bradykinetic phenotype. Next, we analyzed the characteristics of gait (normalized to body weight in order to compensate for the size difference between genotypes). Mutant mice had an increased stride width per body weight index compared to normal controls, suggestive of a significant wide-based gate. This was confirmed by a generalized disorganization of the gait, including dragging marks, changes in direction and freezing (data not shown). In contrast, *Th*-ki mice did not show abnormal stride length, as observed by an unchanged stride length per body weight index compared to controls. In summary, while the catecholamine deficiency increased with age (Figure 2A-D), the severe motor dysfunction was present from the first measurements at 3 weeks onwards, and its severity appeared independent of age.

Marked diurnal fluctuation of motor behavior is a hallmark in patients with THD (Willemsen *et al.*, 2010, Haugarvoll and Bindoff, 2011). To determine whether the motor performance in mutant mice varied throughout the day, we performed the bar test at 8 a.m. and 8 p.m. in the same set of animals and found that *Th*-ki mice performed significantly better after the resting period (at 8 p.m., note the inverted circadian rhythms of mice compared to humans) than after the activity period (at 8 a.m.), while wt controls presented a stable performance at both times (Willemsen *et al.*, 2010, Haugarvoll and Bindoff, 2011) (Figure 4).

Gradual reduction of TH protein and activity in brain of *Th*-ki mice, with specific loss of TH in striatum

Gene expression of *Th*, *Tph*1 and *Tph*2 (mRNAs) in whole brain extracts of *Th*-ki mice was similar to that in wt mice at different ages, and no particular heterogeneity was observed for transcript numbers in either mice. *Th*-mRNA transcripts (but not *Tph*1 and *Tph*2 mRNAs) showed an increase of about 50% from newborn (1 day) to 3 weeks for both wt and *Th*-ki mice (Supplementary Table S1). On the other hand, immunoquantification of TH protein content in whole brain extracts showed a remarkable 5-fold increase in TH relative to total protein from newborn to 3 weeks in normal mice, but no significant increase in TH protein was measured in this period for *Th*-ki (Figure 5A,B). For wt mouse TH content was maintained from 3 weeks up to 1 year, but *Th*-ki revealed a gradual loss of TH protein relative to the normal (wt) content, reaching a value as low as ~3% of wt TH protein in 1 year old animals (Figure 5B, inset). The specific TH activity in brain extracts under standard conditions - measured by a sensitive radiochemical assay (Reinhard *et al.*, 1986) – also followed a similar development as the protein content for the wt animals (the activity increased from 1.6 ± 0.6 to 5.3 ± 1.0 pmol L-Dopa/mg/min from day 1 to 3 weeks, a value that was maintained up to 1 year). However, the activity in *Th*-ki brain extracts was below the sensitivity threshold and could not be determined accurately by the radiochemical assay or other methods tested, including HPLC and fluorimetric detection of L-Dopa (Haavik and Flatmark, 1980).

Loss of TH was also observed by immunohistochemical staining for TH of the *substantia nigra pars compacta* (SNpc) and *ventral tegmental* area (VTA) region and *corpus striatum* on coronal brain sections from perfused adult male *Th*-ki and wt mice (6-7 months old). As seen in Figure 5C we observed a similar expression pattern of TH in *Th*-ki and control mice in the SNpc/VTA, with some less dense stained projections, whereas in the *corpus striatum* we observed an almost complete lack of immunoreactive processes. Furthermore, higher magnification photomicrographs depict a similar soma staining in the midbrain of mutants and controls whereas reduced staining of processes is again observed for the mutants (Figure 5D). A semi-quantitative TH+ cell count performed in the SNpc/VTA of mutant and control brains indicated no decrease of immunoreactive TH cells in the midbrain of the mutants

(220.5±35.5 and 232.5±35.5 for *Th*-ki and *Th*-wt mice, respectively). Together with the lack of aberrant amyloid deposition in either midbrain or *corpus striatum*, as indicated by Congo red staining in these brain areas (Figure 5E), the histological results strongly support lack of neurodegeneration in the midbrain of mutant animals. Rather, our results support the reduction in the amount of TH protein measured by immunoquantification and revealed a marked mislocalization of TH, consistent with a defective transport of mTH-R203H across the nigrostriatal projection (see below).

The misfolding loss-of-function mutations hTH1-R202H and mTH-R203H are not stabilized by DA

In order to understand better the TH dysfunction in THD patients and in *Th*-ki mice, we studied the molecular and kinetic effects of the mutation in the human (h) and mouse (m) TH enzymes, using purified, tetrameric, recombinant hTH1-wt, mTH-wt, hTH1-R202H and mTH-R203H. First we analyzed the substrate and cofactor dependent activity of each enzyme (Figure 6A,B); the steady state activity constants are summarized in Table 1. Compared with hTH1-wt, mTH-wt showed reduced specific activity, but a similar $K_m(BH_4)$, slightly decreased $S_{0.5}$(L-Tyr) (higher substrate affinity for L-Tyr) and reduced substrate inhibition constant (K_{si}), denoting stronger substrate inhibition. The mutants hTH1-R202H and mTH-R203H showed decreased V_{max} and $K_m(BH_4)$ and slight increase of $S_{0.5}$(L-Tyr) compared with their corresponding wt counterparts, indicating a clear, but not severe kinetic defect. On the other hand, an evident destabilizing misfolding of the mutant enzymes was indicated by a 10-fold lower yield of purified tetrameric mutant enzymes expressed in *E. coli*, compared with the wt forms. Decreased protein stability of the hTH1-R202H mutant is also predicted by the FoldX algorithm (Schymkowitz *et al.*, 2005), which estimated a destabilization energy of 9.96 kcal/mol (ΔΔG) based on the tetrameric structure of hTH (PDB 2XSN), including the catalytic and tetramerization domains. To corroborate that the mutation caused the destabilization, we performed differential scanning fluorimetry (DSF) analyses. This method was chosen due to the small amounts of protein required, since protein was limited for the mutants. The mutant enzymes showed reduced stability compared with the respective wt-forms (2-3°C decreased midpoint denaturation (T_m)-values; Figure 7A). Although significant, the decreased thermodynamic stability caused by the mutation could not, however, fully explain the relative decay of TH protein in the *Th*-ki compared to the wt mouse (Figure 5). Additional defects in regulatory stabilization of the mutant mTH-R203H enzyme might explain this relative loss of TH protein in the mutant mouse. Stabilization of TH by DA and other catecholamines is an important regulatory mechanism, which leads to competitive inhibition of TH activity versus the BH_4 cofactor, and provides a natural chaperone effect that prevents degradation of the enzyme (Okuno and Fujisawa, 1991, Sumi-Ichinose *et al.*, 2001, Thöny *et al.*, 2008). *In vitro*, this stabilization is manifested by an increase in the T_m-values and a decrease in its susceptibility to proteolysis (Martinez *et al.*, 1996, McCulloch and

Fitzpatrick, 1999). As expected, hTH1-wt and mTH-wt were stabilized by DA binding, increasing their T_m-values up to 3°C (Figure 7A,B), but the mutants were not stabilized by DA (Fig. 7C,D). In addition, DA protected the wt enzymes, but not the mutants, from limited tryptic proteolysis (shown for hTH1 in Figure 7E-J).

Non-responsiveness of *Th*-ki mice to L-Dopa treatment

We determined the effect of chronic and acute L-Dopa treatment on the motor outcome of juvenile or young adult *Th*-ki mice and controls. In the chronic tests, catalepsy and motor coordination were investigated after daily L-Dopa (plus carbidopa) or mock treatment from birth to 3 weeks of age using a high dose according to recommendations for THD in humans (i.e. 10 mg/kg/day of L-Dopa (Willemsen *et al.*, 2010)). No significant differences were found either in the bar test or rotarod performance in *Th*-ki mice given L-Dopa or vehicle (see Supplementary Figures S5A-B). Similar negative results were obtained from treating adult *Th*-ki mice over a period of 12 days (not shown). Nevertheless, monoamine neurotransmitter analysis in brain extracts of sacrificed mice showed significant *metabolite* improvement following L-Dopa treatment (Figure 8A), although TH protein was certainly not increased (Fig. 8B). Similarly, in an acute test for motor coordination (rotarod) and catalepsy or rigidity (bar test) upon a single dose of L-Dopa (10 mg per kg body weight plus carbidopa), *Th*-ki mice did not show any differences in performance before and 20-45 min after administration (see Supplementary Figures S5C-D), corroborating non-responsiveness of *Th*-ki mice to L-Dopa treatment.

Discussion

The *Th*-ki mouse was generated to provide an experimental *in vivo* model to investigate TH and catecholamine deficiency both in terms of disease pathogenesis and the effect of mutations on enzyme function and regulation *in vivo*. In the longer term, this model appears valuable to test treatments aimed at improving diseases related to loss of DA. The model is clinically robust. The *Th*-ki mouse appears normal at birth, but thereafter exhibits moderate failure to thrive, motor abnormalities including abnormal body posture and twitching, i.e. dystonia-like features, reduced coordination, hypokinesia, ataxia and catalepsy or rigidity-akinesia. There is also clear diurnal variation of the motor defects and lowered blood pressure, as also found in THD patients homozygous for p.Arg233His (Willemsen *et al.*, 2010). The biochemical and other abnormalities in the *Th*-ki mice include an early and persistent decrease in brain DA and noradrenaline to critically low levels, associated with low brain TH, which together with a reduced body weight and hyperprolactinemia are characteristics of THD. *Th*-ki mice were notably homogeneous with respect to all parameters determined in this work, including motor dysfunction, biochemical phenotype and unresponsiveness to L-Dopa, which probably reflects the genetic background homogeneity of these inbred strains. Patients homozygous for p.Arg233His actually show higher phenotypic variability (Willemsen *et al.*, 2010), which might point to THD as a complex trait autosomal recessive disorder where the phenotype might be modulated at different steps of the catecholaminergic systems, reflecting a higher complexity in human than mice.

Previous mice models have not mirrored THD to the same degree as the here presented *Th*-ki mouse. Both the $Th^{-/-}$ and the dopamine β-hydroxylase deficient $Dbh^{-/-}$ knock-out mice have a high pre- and perinatal mortality due to cardiovascular failure associated with the lack of norepinephrine, and confirm the importance of catecholamines for fetal development (Kobayashi *et al.*, 1995, Thomas *et al.*, 1995, Zhou *et al.*, 1995). TH function and norepinephrine synthesis could be rescued in noradrenergic neurons of transgenic $Th^{-/-}$ mice. These DA-deficient mice survive for a short period without treatment (Willemsen *et al.*, 2010, Garcia-Cazorla and Duarte, 2014), but have normal norepinephrine levels and are thus imperfect models for THD. The aromatic amino acid decarboxylase knock-out mouse is catecholamine-deficient and shows a 50% survival, but shows in addition seriously reduced serotonin levels (Lee *et al.*, 2013) and are also not a model to investigate the pathogenic mechanisms of specific TH deficiency.

Newborn *Th*-ki mice show normal values of catecholamines and other metabolites, except for a reduction in HVA. By 3 weeks of age, however, we observed a drop in brain norepinephrine that, despite its crucial role in mouse fetal development (Thomas *et al.*, 1995), did not affect pups survival. Initially, the reduction in norepinephrine was not accompanied by any significant decrease in DA pointing to compensatory mechanisms that maintain DA levels,

e.g. by down-regulation of its degradation (Tunbridge *et al.*, 2006). Concomitant to their defective brain noradrenaline content, *Th*-ki mice fail to accomplish the 5-fold increase in TH protein observed for the *Th*-wt from newborn to 3 weeks (Figure 5B) despite the presence of normal (similar to wt) levels of *Th*-mRNA (Table S1). A similar substantial increase in TH in the same postnatal period has been reported, and this increase appears critical for the correct development of the dopaminergic system and the psychomotor function (Homma *et al.*, 2011). This finding is supported by our results showing early and persistent motor dysfunction in the *Th*-ki mice. The postnatal increase in TH protein in normal mice is not only driven by upregulated transcription (Table S1) but through stabilization of the TH protein, where both the level of BH_4 and catecholamines themselves have been shown to be implicated in the stabilization (Homma *et al.*, 2011, Homma *et al.*, 2013). BH_4 levels are similar in *Th*-wt and knock-in mice, and the $K_m(BH_4)$ for the mutant enzymes indicate a relative high affinity for the cofactor (Table 1). Catecholamine binding and feedback inhibition of TH occur in competition with BH_4 (Nagatsu, 1995, Daubner *et al.*, 2011), and thus the enzyme kinetics data are in accord with a mutation-associated structural change in TH that leads to opposite effects for BH_4 and DA, and to defective stabilization by DA (or norepinephrine; data not shown). Despite some recent insights on residues important for catecholamine binding at the catalytic domain (Briggs *et al.*, 2014), a structural explanation for the defective stabilization by DA in the mutants must await the determination of high resolution structures of full-length TH, including the regulatory domain, where the determinants for high affinity binding are located (McCulloch and Fitzpatrick, 1999, Nakashima *et al.*, 1999). The hTH1-R202H and mTH-R203 mutants show both kinetic (Table 1) and stability defects (Figure 6), but the lack of DA-stabilization of mutant TH emerges as a deleterious regulatory deficiency that explains the lack of accumulation of TH protein in the critical postnatal period in the *Th*-ki mice (Figure 5A,B). Defective stabilization by catecholamines may also support the specific deficit of TH expression in the striatum (Figure 5C,D) since proper transport of TH to this brain area also requires the stabilization of the enzyme (Homma *et al.*, 2013). Mutation associated defective trafficking and aberrant localization of protein cargos is a recurrent pathological mechanism in neurological and neurodegenerative disorders (Hung and Link, 2011, Encalada and Goldstein, 2014). Little is known about mechanisms of transport of TH and dopamine in the dopaminergic nigrostriatal pathway projecting from the SNpc to the caudate-putamen (striatum), although it is accepted that at least in adrenergic neuronal systems TH is fast transported along the axon in an anterograde fashion to the terminals (Brimijoin and Wiermaa, 1977). Accordingly, impaired axonal transport of TH in dopaminergic projections has recently been shown to be associated with parkinsonism and drastic reduction of TH and DA levels in striatal synapses (Ittner *et al.*, 2008). It is thus very probable that the observed motor dysfunction in the *Th*-ki mice is caused by defective TH transport leading to scarce TH and DA in synaptic terminals to activate DA receptors in the caudate-putamen.

Lack or poor responsiveness to L-Dopa is manifested by a large number of patients with THD type B, particularly those with the hTH1-R202H mutation (Grattan-Smith *et al.*, 2002, Willemsen *et al.*, 2010). One interesting finding of the present study is that the motor dysfunction of the *Th*-ki mice is not improved by standard L-Dopa supplementation even when treated from the first day of life. Other mouse models with DA deficiency show a partial recovery with DA treatment, especially in features such as feeding problems. Motor improvement is, however, often incomplete (Zhou and Palmiter, 1995), reflecting perhaps the developmental deficiencies in the fetal and perinatal periods (Zhou and Palmiter, 1995, Homma *et al.*, 2011). Possible neurodevelopment disorders associated to defective stabilization by catecholamines and consequent mislocalization of TH cannot be ruled out as the reason for the lack of Dopa-responsiveness of the motor dysfunction in the *Th*-ki mice, despite the apparent correction of L-Dopa levels and increase of DA in brain extracts observed after treatment (Figure 8A). Developing novel non-L-Dopa-based therapeutic strategies for THD type B may thus be an attractive approach, especially for patients with the specific h*TH*-R233H mutation. In this respect, emerging therapies based on protein stabilization, e.g. pharmacological chaperones, appear promising, as we have previously shown in in vitro experiments that the variant hTH1-R202H can be stabilized by compounds with chaperone potential (Calvo *et al.*, 2010)(Hole *et al.,* 2015). Furthermore, the diurnal fluctuation of motor deficits is definitively an important hallmark of our *Th*-ki mutant mouse and may also be exploited in the search for novel treatment strategies based on the restorative potential of either circadian regulation of TH activity and/or restorative properties of sleep.

Finally, the growth retardation measured in the *Th*-ki mutant mouse in combination with normal food intake, normoglycemia and apparent reduced energy expenditure in the metabolic cage deserves explanation. Surviving mice with selective DA-deficiency in dopaminergic neurons, but not in noradrenergic neurons, exhibit abnormal feeding behavior including swallowing difficulties (aphagy) (Zhou and Palmiter, 1995, Szczypka *et al.*, 1999), symptoms we did not observe in the *Th*-ki mice. On the other hand, growth retardation in combination with normal food intake has also previously been found in total and neuron specific DA-receptor knock-out mice which shows reduced DA signaling (Baik *et al.*, 1995, Noain *et al.*, 2013). Like these other surviving TH-deficient mice with reduced noradrenergic activity, the here presented *Th*-ki mice showed lowered resting metabolic rate with respect to wt mice. Furthermore, it has become increasingly clear that isolated dopaminergic abnormalities and parkinsonian syndromes involve abnormal or increased energy expenditure during walking and motor tasks which may explain the reduction in growth of mutant mice despite comparable food intake with wt mice (Molero-Luis *et al.*, 2013, Amano *et al.*, 2014)).

In conclusion, there is a large spectrum of phenotypes in patients with THD, resulting from diverse deficiencies in absolute and relative DA and norepinephrine levels with different impact on systemic and motor function (Willemsen *et al.*, 2010). This variability would depend on the catalytic, conformational and regulatory defects of the particular TH mutation. In agreement with severely affected patients homozygous for the mutation p.R233H, *Th*-ki mice studied in this work present severe motor deficiencies from a juvenile age onwards, and these abnormalities are apparently not corrected by classical replacement treatment with L-Dopa. The mutant hTH1-R202H and mTH-R203H proteins are not stabilized by DA, leading to intracellular instability, gradual loss of TH activity and altered *nigro-striatal* distribution, aiding to interpret the biochemical and locomotor phenotype of *Th*-ki. In addition to contribute to the understanding of the biochemical pathogenesis of catecholamine deficiency this mouse model offers a useful platform for designing and evaluating new routes to disease therapies not only for THD, but also other genetic and idiopathic dopaminergic deficiencies.

Acknowledgments

This work was supported by grants from the Hartmann Müller Stiftung für wissenschaftliche Forschung der Universität Zürich (to BT), the Neuroscience Center Zurich (to BT), The Research Council of Norway, the Western Regional Health Authorities and the K. G. Jebsen Foundation (to AM). We thank Flurin Item for metabolic cage analyses and the Division of Clinical Chemistry and Biochemistry at the University Children's Hospital Zürich for sharing technical equipment, and the Animal Facilities (BZL) of the University Hospital Zürich for animal maintenance and support.

The authors have declared that no conflict of interest exists

References

Aitkenhead H, Heales SJ. Establishment of paediatric age-related reference intervals for serum prolactin to aid in the diagnosis of neurometabolic conditions affecting dopamine metabolism. Ann Clin Biochem. 2013;50(Pt 2):156-8.

Amano S, Kegelmeyer D, Hong SL. Rethinking energy in parkinsonian motor symptoms: a potential role for neural metabolic deficits. Frontiers in systems neuroscience. 2014;8:242.

Avale ME, Falzone TL, Gelman DM, Low MJ, Grandy DK, Rubinstein M. The dopamine D4 receptor is essential for hyperactivity and impaired behavioral inhibition in a mouse model of attention deficit/hyperactivity disorder. Mol Psychiatry. 2004;9(7):718-26.

Baik JH, Picetti R, Saiardi A, Thiriet G, Dierich A, Depaulis A, et al. Parkinsonian-like locomotor impairment in mice lacking dopamine D2 receptors. Nature. 1995;377(6548):424-8.

Bello EP, Mateo Y, Gelman DM, Noain D, Shin JH, Low MJ, et al. Cocaine supersensitivity and enhanced motivation for reward in mice lacking dopamine D2 autoreceptors. Nat Neurosci. 2011;14(8):1033-8.

Ben-Jonathan N. Dopamine: a prolactin-inhibiting hormone. Endocr Rev. 1985;6(4):564-89.

Bjorklund A, Dunnett SB. Dopamine neuron systems in the brain: an update. Trends in neurosciences. 2007;30(5):194-202.

Blau N, Thony B, Renneberg A, Penzien JM, Hyland K, Hoffmann GF. Variant of dihydropteridine reductase deficiency without hyperphenylalaninaemia: effect of oral phenylalanine loading. Journal of inherited metabolic disease. 1999;22(3):216-20.

Bohnen NI, Jahn K. Imaging: What can it tell us about parkinsonian gait? Mov Disord. 2013;28(11):1492-500.

Bornstein SR, Tian H, Haidan A, Bottner A, Hiroi N, Eisenhofer G, et al. Deletion of tyrosine hydroxylase gene reveals functional interdependence of adrenocortical and chromaffin cell system in vivo. Proceedings of the National Academy of Sciences of the United States of America. 2000;97(26):14742-7.

Briggs GD, Bulley J, Dickson PW. Catalytic domain surface residues mediating catecholamine inhibition in tyrosine hydroxylase. Journal of biochemistry. 2014;155(3):183-93.

Brimijoin S, Wiermaa MJ. Rapid axonal transport of tyrosine hydroxylase in rabbit sciatic nerves. Brain research. 1977;121(1):77-96.

Calvo AC, Scherer T, Pey AL, Ying M, Winge I, McKinney J, et al. Effect of pharmacological chaperones on brain tyrosine hydroxylase and tryptophan hydroxylase 2. J Neurochem. 2010;114(3):853-63.

Catafau AM, Bullich S. Amyloid PET imaging: applications beyond Alzheimer's disease. Clin Transl Imaging. 2015;3(1):39-55.

Daubner SC, Le T, Wang S. Tyrosine hydroxylase and regulation of dopamine synthesis. Arch Biochem Biophys. 2011;508(1):1-12.

de Medinaceli L, Freed WJ, Wyatt RJ. An index of the functional condition of rat sciatic nerve based on measurements made from walking tracks. Exp Neurol. 1982;77(3):634-43.

Delafontaine P, Song YH, Li Y. Expression, regulation, and function of IGF-1, IGF-1R, and IGF-1 binding proteins in blood vessels. Arterioscler Thromb Vasc Biol. 2004;24(3):435-44.

Eisenhofer G, Kopin IJ, Goldstein DS. Catecholamine metabolism: a contemporary view with implications for physiology and medicine. Pharmacol Rev. 2004;56(3):331-49.

Elzaouk L, Leimbacher W, Turri M, Ledermann B, Burki K, Blau N, et al. Dwarfism and low insulin-like growth factor-1 due to dopamine depletion in Pts-/- mice rescued by

feeding neurotransmitter precursors and H4-biopterin. The Journal of biological chemistry. 2003;278(30):28303-11.

Encalada SE, Goldstein LS. Biophysical challenges to axonal transport: motor-cargo deficiencies and neurodegeneration. Annual review of biophysics. 2014;43:141-69.

Fossbakk A, Kleppe R, Knappskog PM, Martinez A, Haavik J. Functional studies of tyrosine hydroxylase missense variants reveal distinct patterns of molecular defects in dopa-responsive dystonia. Human mutation. 2014;35(7):880-90.

Garcia-Cazorla A, Duarte ST. Parkinsonism and inborn errors of metabolism. J Inherit Metab Dis. 2014;37(4):627-42.

Gelman DM, Noain D, Avale ME, Otero V, Low MJ, Rubinstein M. Transgenic mice engineered to target Cre/loxP-mediated DNA recombination into catecholaminergic neurons. Genesis. 2003;36(4):196-202.

Grattan-Smith PJ, Wevers RA, Steenbergen-Spanjers GC, Fung VS, Earl J, Wilcken B. Tyrosine hydroxylase deficiency: clinical manifestations of catecholamine insufficiency in infancy. Movement disorders: official journal of the Movement Disorder Society. 2002;17(2):354-9.

Haavik J, Blau N, Thony B. Mutations in human monoamine-related neurotransmitter pathway genes. Hum Mutat. 2008;29(7):891-902.

Haavik J, Flatmark T. Rapid and sensitive assay of tyrosine 3-monooxygenase activity by high-performance liquid chromatography using the native fluorescence of DOPA. Journal of chromatography. 1980;198(4):511-5.

Haugarvoll K, Bindoff LA. A novel compound heterozygous tyrosine hydroxylase mutation (p.R441P) with complex phenotype. J Parkinsons Dis. 2011;1(1):119-22.

Hole M, Underhaug J, Diez H, Ying M, Røhr ÅK, Jorge-Finnigan A**,** et al. Discovery of compounds that protect tyrosine hydroxylase activity through different mechanisms. Biochim Biophys Acta. 2015, in press.

Homma D, Katoh S, Tokuoka H, Ichinose H. The role of tetrahydrobiopterin and catecholamines in the developmental regulation of tyrosine hydroxylase level in the brain. Journal of neurochemistry. 2013;126(1):70-81.

Homma D, Sumi-Ichinose C, Tokuoka H, Ikemoto K, Nomura T, Kondo K, et al. Partial biopterin deficiency disturbs postnatal development of the dopaminergic system in the brain. The Journal of biological chemistry. 2011;286(2):1445-52.

Hung MC, Link W. Protein localization in disease and therapy. Journal of cell science. 2011;124(Pt 20):3381-92.

Ittner LM, Fath T, Ke YD, Bi M, van Eersel J, Li KM, et al. Parkinsonism and impaired axonal transport in a mouse model of frontotemporal dementia. Proceedings of the National Academy of Sciences of the United States of America. 2008;105(41):15997-6002.

Kobayashi K, Morita S, Sawada H, Mizuguchi T, Yamada K, Nagatsu I, et al. Targeted disruption of the tyrosine hydroxylase locus results in severe catecholamine depletion and perinatal lethality in mice. The Journal of biological chemistry. 1995;270(45):27235-43.

Krege JH, Hodgin JB, Hagaman JR, Smithies O. A noninvasive computerized tail-cuff system for measuring blood pressure in mice. Hypertension. 1995;25(5):1111-5.

Kumer SC, Vrana KE. Intricate regulation of tyrosine hydroxylase activity and gene expression. J Neurochem. 1996;67(2):443-62.

Kunkel-Bagden E, Dai HN, Bregman BS. Methods to assess the development and recovery of locomotor function after spinal cord injury in rats. Exp Neurol. 1993;119(2):153-64.

Kurian MA, Gissen P, Smith M, Heales S, Jr., Clayton PT. The monoamine neurotransmitter disorders: an expanding range of neurological syndromes. The Lancet Neurology. 2011;10(8):721-33.

Lee NC, Shieh YD, Chien YH, Tzen KY, Yu IS, Chen PW, et al. Regulation of the dopaminergic system in a murine model of aromatic L-amino acid decarboxylase deficiency. Neurobiology of disease. 2013;52:177-90.
Livak KJ, Schmittgen TD. Analysis of relative gene expression data using real-time quantitative PCR and the 2(-Delta Delta C(T)) Method. Methods. 2001;25(4):402-8.
Martinez A, Haavik J, Flatmark T, Arrondo JL, Muga A. Conformational properties and stability of tyrosine hydroxylase studied by infrared spectroscopy. Effect of iron/catecholamine binding and phosphorylation. J Biol Chem. 1996;271(33):19737-42.
McCulloch RI, Fitzpatrick PF. Limited proteolysis of tyrosine hydroxylase identifies residues 33-50 as conformationally sensitive to phosphorylation state and dopamine binding. Arch Biochem Biophys. 1999;367(1):143-5.
Molero-Luis M, Serrano M, Ormazabal A, Perez-Duenas B, Garcia-Cazorla A, Pons R, et al. Homovanillic acid in cerebrospinal fluid of 1388 children with neurological disorders. Dev Med Child Neurol. 2013;55(6):559-66.
Nagatsu T. Tyrosine hydroxylase: human isoforms, structure and regulation in physiology and pathology. Essays Biochem. 1995;30:15-35.
Nagatsu T, Levitt M, Udenfriend S. Tyrosine Hydroxylase. The Initial Step In Norepinephrine Biosynthesis. The Journal of biological chemistry. 1964;239:2910-7.
Nakashima A, Mori K, Suzuki T, Kurita H, Otani M, Nagatsu T, et al. Dopamine inhibition of human tyrosine hydroxylase type 1 is controlled by the specific portion in the N-terminus of the enzyme. Journal of neurochemistry. 1999;72(5):2145-53.
Noain D, Perez-Millan MI, Bello EP, Luque GM, Casas Cordero R, Gelman DM, et al. Central dopamine D2 receptors regulate growth-hormone-dependent body growth and pheromone signaling to conspecific males. J Neurosci. 2013;33(13):5834-42.
Obeso JA, Rodriguez-Oroz MC, Goetz CG, Marin C, Kordower JH, Rodriguez M, et al. Missing pieces in the Parkinson's disease puzzle. Nature medicine. 2010;16(6):653-61.
Okuno S, Fujisawa H. Conversion of tyrosine hydroxylase to stable and inactive form by the end products. Journal of neurochemistry. 1991;57(1):53-60.
Reed MC, Lieb A, Nijhout HF. The biological significance of substrate inhibition: a mechanism with diverse functions. Bioessays. 2010;32(5):422-9.
Reinhard JF, Jr., Smith GK, Nichol CA. A rapid and sensitive assay for tyrosine-3-monooxygenase based upon the release of 3H2O and adsorption of [3H]-tyrosine by charcoal. Life Sci. 1986;39(23):2185-9.
Roberts KM, Fitzpatrick PF. Mechanisms of tryptophan and tyrosine hydroxylase. IUBMB life. 2013;65(4):350-7.
Sato K, Sumi-Ichinose C, Kaji R, Ikemoto K, Nomura T, Nagatsu I, et al. Differential involvement of striosome and matrix dopamine systems in a transgenic model of dopa-responsive dystonia. Proceedings of the National Academy of Sciences of the United States of America. 2008;105(34):12551-6.
Schymkowitz J, Borg J, Stricher F, Nys R, Rousseau F, Serrano L. The FoldX web server: an online force field. Nucleic acids research. 2005;33(Web Server issue):W382-8.
Sumi-Ichinose C, Urano F, Kuroda R, Ohye T, Kojima M, Tazawa M, et al. Catecholamines and serotonin are differently regulated by tetrahydrobiopterin. A study from 6-pyruvoyltetrahydropterin synthase knockout mice. The Journal of biological chemistry. 2001;276(44):41150-60.
Suresh Babu R, Sunandhini RL, Sridevi D, Periasamy P, Namasivayam A. Locomotor behavior of bonnet monkeys after spinal contusion injury: footprint study. Synapse. 2012;66(6):509-21.

Swoap SJ, Weinshenker D, Palmiter RD, Garber G. Dbh(-/-) mice are hypotensive, have altered circadian rhythms, and have abnormal responses to dieting and stress. American journal of physiology Regulatory, integrative and comparative physiology. 2004;286(1):R108-13.

Szczypka MS, Rainey MA, Kim DS, Alaynick WA, Marck BT, Matsumoto AM, et al. Feeding behavior in dopamine-deficient mice. Proceedings of the National Academy of Sciences of the United States of America. 1999;96(21):12138-43.

Tank AW, Xu L, Chen X, Radcliffe P, Sterling CR. Post-transcriptional regulation of tyrosine hydroxylase expression in adrenal medulla and brain. Annals of the New York Academy of Sciences. 2008;1148:238-48.

Thomas SA, Matsumoto AM, Palmiter RD. Noradrenaline is essential for mouse fetal development. Nature. 1995;374(6523):643-6.

Thöny B, Calvo AC, Scherer T, Svebak RM, Haavik J, Blau N, et al. Tetrahydrobiopterin shows chaperone activity for tyrosine hydroxylase. J Neurochem. 2008;106:672-81.

Tunbridge EM, Harrison PJ, Weinberger DR. Catechol-o-methyltransferase, cognition, and psychosis: Val158Met and beyond. Biological psychiatry. 2006;60(2):141-51.

Willemsen MA, Verbeek MM, Kamsteeg EJ, de Rijk-van Andel JF, Aeby A, Blau N, et al. Tyrosine hydroxylase deficiency: a treatable disorder of brain catecholamine biosynthesis. Brain. 2010;133(Pt 6):1810-22.

Willemsen MA, Verbeek MM, Kamsteeg EJ, de Rijk-van Andel JF, Aeby A, Blau N, et al. Tyrosine hydroxylase deficiency: a treatable disorder of brain catecholamine biosynthesis. Brain : a journal of neurology. 2010;133:1810-22.

Wueest S, Mueller R, Bluher M, Item F, Chin AS, Wiedemann MS, et al. Fas (CD95) expression in myeloid cells promotes obesity-induced muscle insulin resistance. EMBO Mol Med. 2014;6(1):43-56.

Yeung WL, Lam CW, Hui J, Tong SF, Wu SP. Galactorrhea-a strong clinical clue towards the diagnosis of neurotransmitter disease. Brain Dev. 2006;28(6):389-91.

Zhou QY, Palmiter RD. Dopamine-deficient mice are severely hypoactive, adipsic, and aphagic. Cell. 1995;83(7):1197-209.

Zhou QY, Quaife CJ, Palmiter RD. Targeted disruption of the tyrosine hydroxylase gene reveals that catecholamines are required for mouse fetal development. Nature. 1995;374(6523):640-3.

Zigmond RE, Schwarzschild MA, Rittenhouse AR. Acute regulation of tyrosine hydroxylase by nerve activity and by neurotransmitters via phosphorylation. Annual review of neuroscience. 1989;12:415-61.

FIGURES

Figure 1. Sex-specific differences in body weight between wt and *Th*-ki mice. (**A**) Female and (**B**) male mice fed *ad libitum* with standard chow. Growth retardation resulted in reduced body weight, for instance at the age of 12 weeks 25% reduction for females and 34% reduction for males. Significant differences between *Th*-ki and wt combined with heterozygotes mice are indicated: **, $p<0.01$; ***, $p<0.001$ (Student's two tailed *t*-test).

Figure 2. Gradual loss of brain monoamine neurotransmitter metabolites in *Th*-ki mice. **(A)** Newborn mice, 1 day, **(B)** juvenile mice, 3 weeks, **(C)** adult mice, 12 weeks, and **(D)** adult mice, 1 year. *Th*-wt mice are shown in black and *Th*-ki in gray. Monoamine neurotransmitter metabolites are depicted in pmol/mg of total brain protein. 3-OMD, 3-*O*-methlydopa; MHPG, 3-methoxy-4-hydroxyphenylethylene glycol; HVA, homovanillic acid; 5-HTP, 5-hydroxytryptophane; 5-HIAA, 5-hydroxyindoleacetic acid. Significant difference from the corresponding wt value is indicated by asterisks: *, $p<0.05$; **, $p<0.01$; ***, $p<0.001$ (Student's two tailed *t*-test).

Figure 3. Motor function tests of mutant (*Th*-ki) and wt (*Th*-wt) male mice at different ages. (A) Bar test for assessment of catalepsy. **(B)** Rotarod test for determination of motor coordination. **(C)** Total distance travelled in the open field test. **(D)** Mean velocity of locomotion in the open field test. **(E)** Gait analysis to test for stride width normalized to body weight. **(F)** Gait analysis to test for short-step disorder (stride length normalized to body weight). *Th*-wt mice are shown in black and *Th*-ki in gray. Significant difference from the corresponding wt value is indicated: **, $p<0.01$; ***, $p<0.001$ (Student's two tailed *t*-test or ANOVA for fluctuation bar test).

Figure 4. The bar test for catalepsy reveals diurnal fluctuation of motor deficits. Bar test performed at 8 a.m. (black bars) and 8 p.m. (grey bars) to explore potential fluctuations in catalepsy severity. While there was no difference for *Th*-wt mice performance at different day times, *Th*-ki mice exhibited a significant difference between morning and evening (*$p<0.05$; two-way ANOVA for fluctuation bar test). The overall difference between genotypes confirms the results shown in Figure 3A (indicated by the three asterisks; ***, $p<0.001$; Student's two tailed *t*-test).

Figure 5. TH protein content in brain from *Th*-wt and *Th*-ki mice. (A) Representative immunoblots of brain extracts of mice at the age of 1 day, 3 weeks, 12 weeks and 1 year; kDa, standard; mTH, purified mouse TH; wt (*Th*-wt) and ki (*Th*-ki) mice. **(B)** TH protein content in brain extracts from *Th*-wt (black bars) and *Th*-ki mice (grey bars), as density of the 59 kDa TH band relative to the intensity of the GAPDH band. Inset: % of TH protein content (grey

bars) in brain extracts of *Th*-ki vs. *Th*-wt mice. Significant difference between mice at different ages with mice at 1 day is indicated: *, p<0.001 (Student's two tailed *t*-test). **(C-E)** Immunohistochemical and Congo red staining of TH in brain of *Th*-wt and *Th*-ki mutant mice, at the age of 6-7 months. **(C)** *Substantia nigra pars compacta* (SNpc)/ventral tegmental area (VTA) of *Th*-wt and *Th*-ki mice present a similar degree of staining indicating lack of neuro-degeneration in the mutant mice, while a striking lack of TH staining was observed in the *corpus striatum* in *Th*-ki mice compared to wt control mice, indicating a largely reduced amount of TH protein in these neuronal processes. **(D)** Higher magnification view of midbrain TH+ cell bodies at different levels (top and middle panels) and inset images depicting the higher density of processes staining in *Th*-wt compared to *Th*-ki brains (bottom panel). **(E)** Congo red staining in mutant and wt controls. The scale bars represent ~0.5 mm (C, E left), ~1.1 mm (E, right), and ~100 μm (D).

Figure 6. Steady-state kinetics characterization of recombinant purified human TH1 (hTH1) and mouse TH (mTH), and the respective mutants R202H and R203H. Specific activity of hTH1-wt (●), mTH-wt (○), hTH1-R202H (▼) and mTH-R203 (Δ) measured **(A)** at different concentrations of the cofactor BH_4 (0−1000 μM) and fixed L-tyrosine (L-Tyr) concentration (25 μM), and **(B)** at different concentrations of L-Tyr (0−200 μM) and fixed BH_4 (200 μM). Results are means ± S.D. for three different experiments.

Figure 7. The stability of recombinant purified human TH1 (hTH1) and mouse TH (mTH) and the respective mutants R202H and R203H, and effect of DA. (A-D) Differential scanning fluorimetry profiles (fluorescence at 610 nm vs. temperature) for hTH1-wt **(A)**, mTH-wt **(B)**, hTH1-R202H **(C)** and mTH-R203 **(D)**, analyzed at a concentration of 0.9 μM subunit without (solid black line) and with (dotted line) equimolar amount (0.9 μM) of DA. The midpoint denaturation (T_m)-values, determined as maximal temperature in first-derivatives, are shown in the corresponding plots. **(E)** SDS-PAGE showing the limited tryptic digestion of hTH1-wt (lanes 1-5) and hTH1-R202H (lanes 6-10) in the absence (2,3,7,8) and the presence (4,5,9,10) of 50 μM DA; 1 and 6 are the respective controls in the absence of trypsin. Conditions: 2.5 μM subunit hTH1 or hTH1-R202H were incubated with trypsin for 30 s (2,4,7,9) or 60 s (3,5,8,10) at 25°C, at a TH:trypsin ratio of 200:1. The gels were stained with Coomassie Brilliant Blue and the raw area of the bands was measured using the Image Lab 3.0.1 software, and represented for lanes 1, 3, 5, 6, 8 and 10 in **F**, **G**, **H**, **I**, **J** and **K**, respectively. At the selected conditions, hTH1-wt (apparent molecular weight of 59 kDa), was trypsinized into two truncated forms of 57 and 54 kDa, both lacking the N-terminal peptide MPTPDATTPQAKGFR (analyses by LC–MS/MS spectroscopy; data not shown).

Figure 8. Outcome of L-Dopa treatment of *Th*-ki mice on brain monoamine neurotransmitter metabolites and TH protein. Mutant *Th*-ki and *Th*-wt mice were treated from day 1 after birth onwards for a period of 3 weeks with L-Dopa (10 mg/kg/day) plus carbidopa (2.5 mg/kg/day) or vehicle (ddH_20 control); inset: L-dopa in pmol/mg protein. **(A)** Brain monoamine neurotransmitter metabolites. **(B)** TH protein relative to GAPDH is shown for *Th*-wt and *Th*-ki mice with or without L-Dopa/carbidopa treatment. In both A and B, significant difference from the corresponding wt value is indicated: *, $p<0.05$; **, $p<0.01$; ***, $p<0.001$ (Student's two tailed *t*-test).

SUPPLEMENTARY FIGURES

Suppl. Figure S1. Generation of the *Th*-ki mouse. (A) Schematic representation of the *Th*-ki mouse gene containing 13 exons with the *Th*-wt allele R203 in exon 5 (in red; the gene is not drawn to scale; NCBI gene ID 21823, transcript variant *Th*-1 NM_0093771.1; Ensembl gene ID ENSMUSG00000000214). The targeting vector contains a 3.8 kb short homology arm (SHA) and a 6.1 kb long homology arm (LHA), including the mouse R203H mutation in exon 5'. At the bottom, the targeted mutant *Th*-ki allele is shown with location of primers for PCR-genotyping (see below). For validation of correct recombination, Southern blot analyses were performed (supplied upon request). FRT, flippase recognition target site; NeoR, neomycin resistance gene for positive selection; TK, thymidine kinase gene for negative selection. **(B)** Details of the DNA sequence of exon 5 of the wt (left) and mutant (right) alleles. The wt sequence of the R203 codon overlaps with a *Hae*II endonuclease recognition site which is destroyed in the mutant allele R203H. **(C)** Conventional 2% agarose gel of representative PCR-genotyping for the *Th*-ki allele with a size difference of 85 bp due to the additional FRT site in the *Th*-ki allele which is in *cis* with the R203H mutation. Position of the primer pair is indicated in A (for more details see Materials and Methods).

Suppl. Figure S2. Similar food intake and respiratory exchange ratio but reduced energy expenditure and locomotor activity during the dark period in *Th*-ki compared to *Th*-wt mice. Food intake **(A)**, respiratory exchange ratio **(B)**, locomotor activity **(C)** and energy expenditure **(D)** were determined in an open-circuit indirect calorimetry system equipped with an infrared light-beam and a feeding monitor system as described in Materials and Methods. After mice were adapted to single caging, data were obtained during a 24-h period in *Th*-wt (black bars) and *Th*-ki (grey bars) mice and results are depicted either over the whole 24-h period or separated into light and dark phase (n = 4-5). Error bars represent SEM. *, $p<0.05$; **, $p<0.01$; ***, $p<0.001$ (Student's *t*-test).

Suppl. Figure S3. Serum parameters including total thyroxine (tT4), IGF-1 and prolactin, as well blood pressure measurements in wt and *Th*-ki mice. **(A)** Serum total tT4 (nM), **(B)** systolic blood pressure (mm of Hg), **(C)** serum IGF-1 (ng/ml), and **(D)** serum prolactin (ng/ml), in *Th*-wt (black bars) and *Th*-ki mice (grey bars); the number of mice per group is indicated. Significant difference is indicated: *, $p<0.05$ (Student's two tailed *t*-test).

Suppl. Figure S4. Biopterin content in whole brain extracts (in pmol/mg of total protein) at different ages of *Th*-wt and *Th*-ki mice. See text for details.

Suppl. Figure S5. Bar and rotarod tests in *Th*-wt and *Th*-ki mutant mice after chronic (A-B) and acute (C-D) treatment with L-Dopa. **(A, C)** Bar test to assess catalepsy, and **(B, D)** rotarod test to determine motor coordination. For (**A-B**), *Th*-ki and *Th*-wt mice were treated after birth for a period of 3 weeks with L-Dopa (10 mg/kg/day) plus carbidopa (2.5 mg/kg/day), or with vehicle. For (**C-D**), all mice were first tested after vehicle administration, and subsequently, fed per os a single dose of L-Dopa (10 mg/kg) plus carbidopa (2.5 mg/kg), and re-tested 20-45 min after administration. Results from treatment with ddH_20 (vehicle) or L-Dopa/carbidopa are shown in black or black-white stripes for *Th*-wt mice, and in gray or gray-white stripes for *Th*-ki mice. Significant differences from the corresponding wt values are indicated: ***, $p<0.001$ (Student's two tailed *t*-test).

Table 1. Steady-state kinetic parameters for recombinant purified human TH1 (hTH1) and mouse TH (mTH) wild-type (wt) forms, and the respective mutants hTH1-R202H and R203H. See also Figure 6. Results are means ± S.D. for three different experiments.

Enzyme	BH_4		L-Tyr	
	V_{max} (nmol of L-dopa/min×mg)	K_m (BH_4) (µM)	V_{max} (nmol of L-dopa/min×mg)	$S_{0.5}$(L-Tyr) (µM)	K_{si}[1] (µM)
hTH1-wt	400 ± 11	50 ± 6	782 ± 41	22 ± 1	54 ± 5
mTH-wt	252 ± 14[2*]	47 ± 10	583 ± 46[2*]	15 ± 1[2*]	28 ± 4[2*]
hTH1-R202H	162 ± 3[2*]	34 ± 3[2*]	344 ± 50[2*]	28 ± 3	60 ± 9
mTH-R203H	132 ± 3[3*]	21 ± 2[3*]	280 ± 40[3*]	23 ± 5	49 ± 6[3*]

For BH_4 concentration dependency, data were fit to the Michaelis-Menten model and for L-Tyr concentration dependency to the substrate inhibition model.

[1]K_{si}, substrate inhibition constant
[2]*, p< 0.05 with respect to corresponding values for hTH1-wt
[3]*, p< 0.05 with respect to corresponding values for mTH-wt

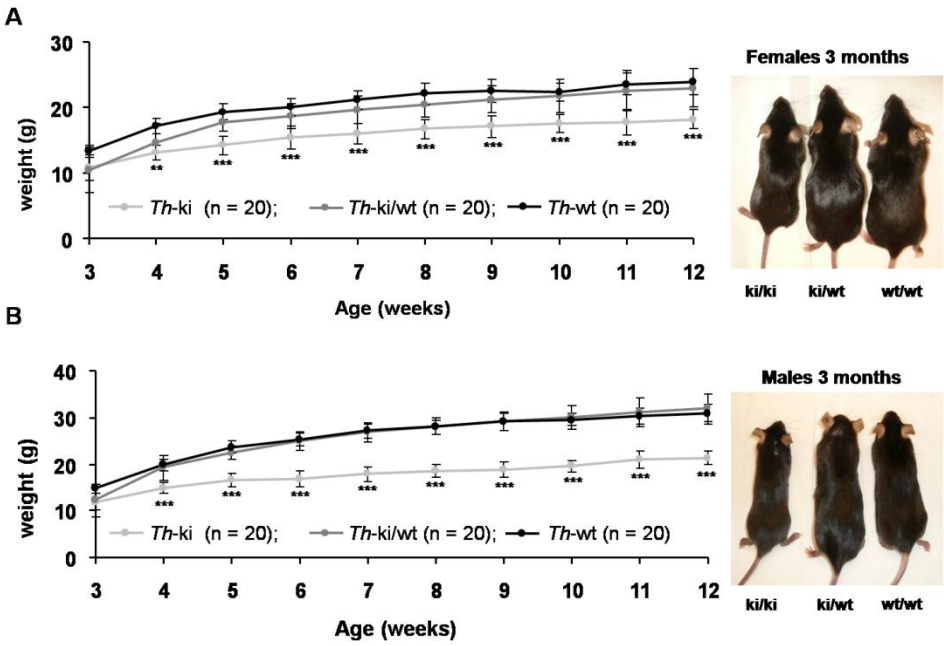

Fig. 1A-B, Körner et al

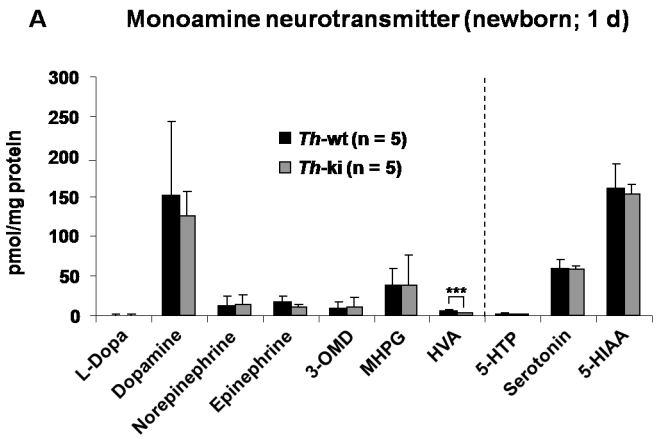

Fig. 2A, Korner et al

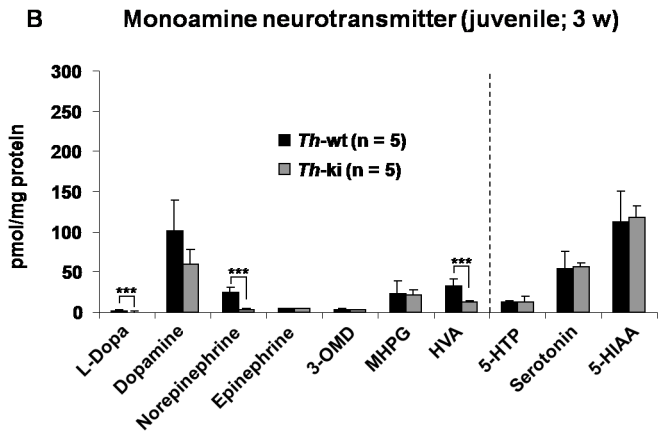

Fig. 2B, Korner et al

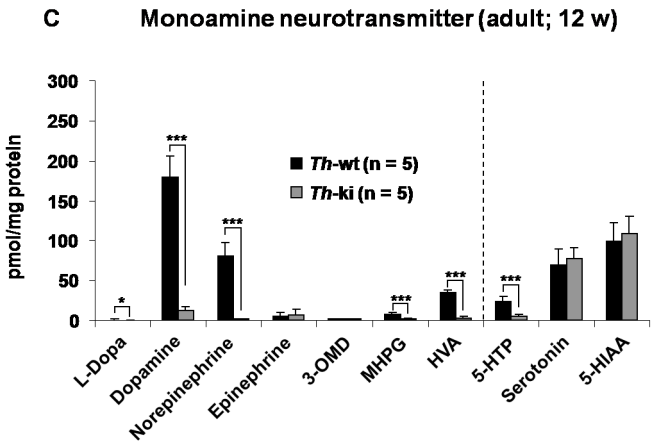

Fig. 2C, Korner et al

D Monoamine neurotransmitter (adult; 1 y)

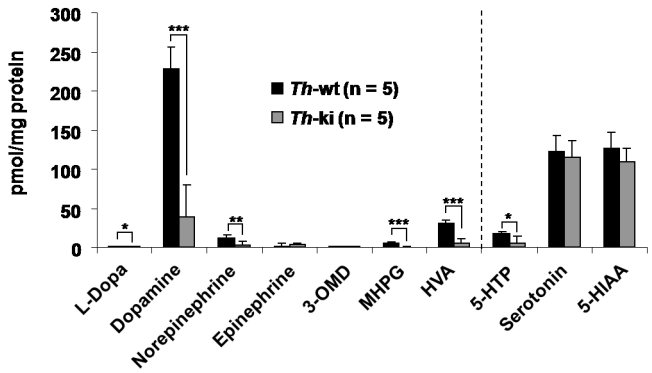

Fig. 2D, Korner et al

A **Bar test: catalepsy**

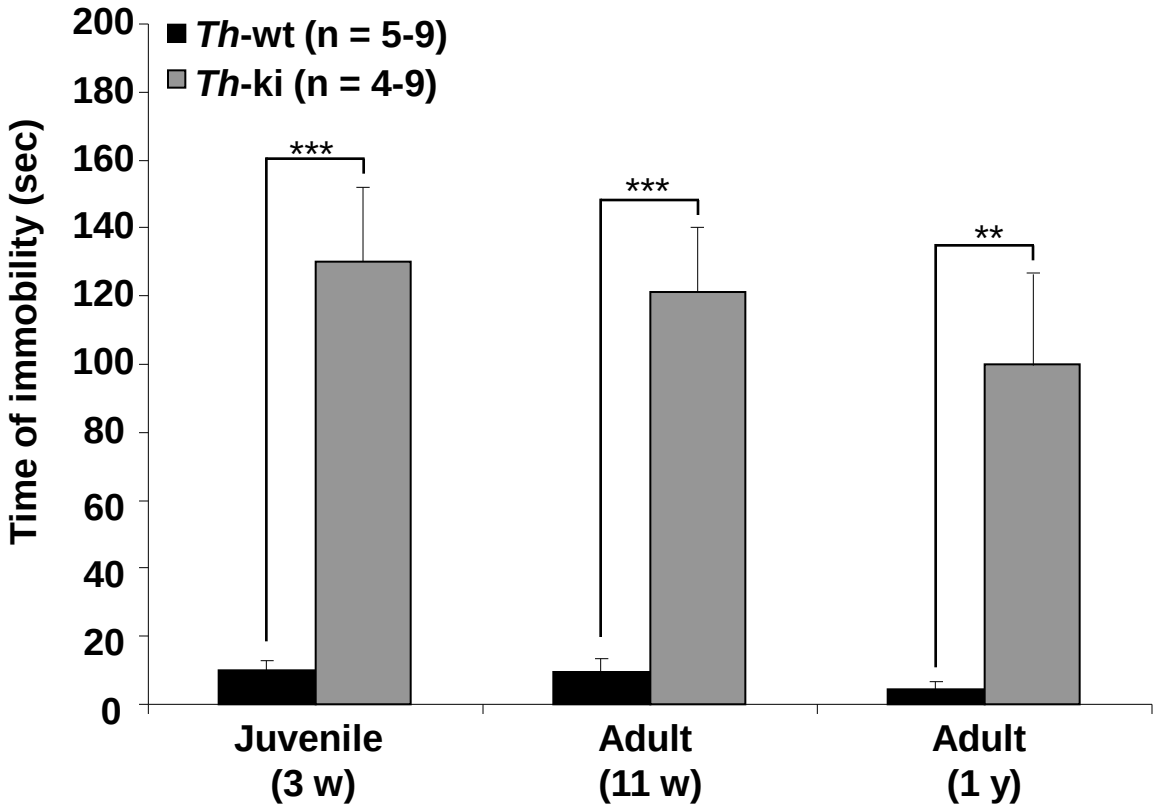

Fig. 3A, Korner et al

B **Rotarod test: motor coordination**

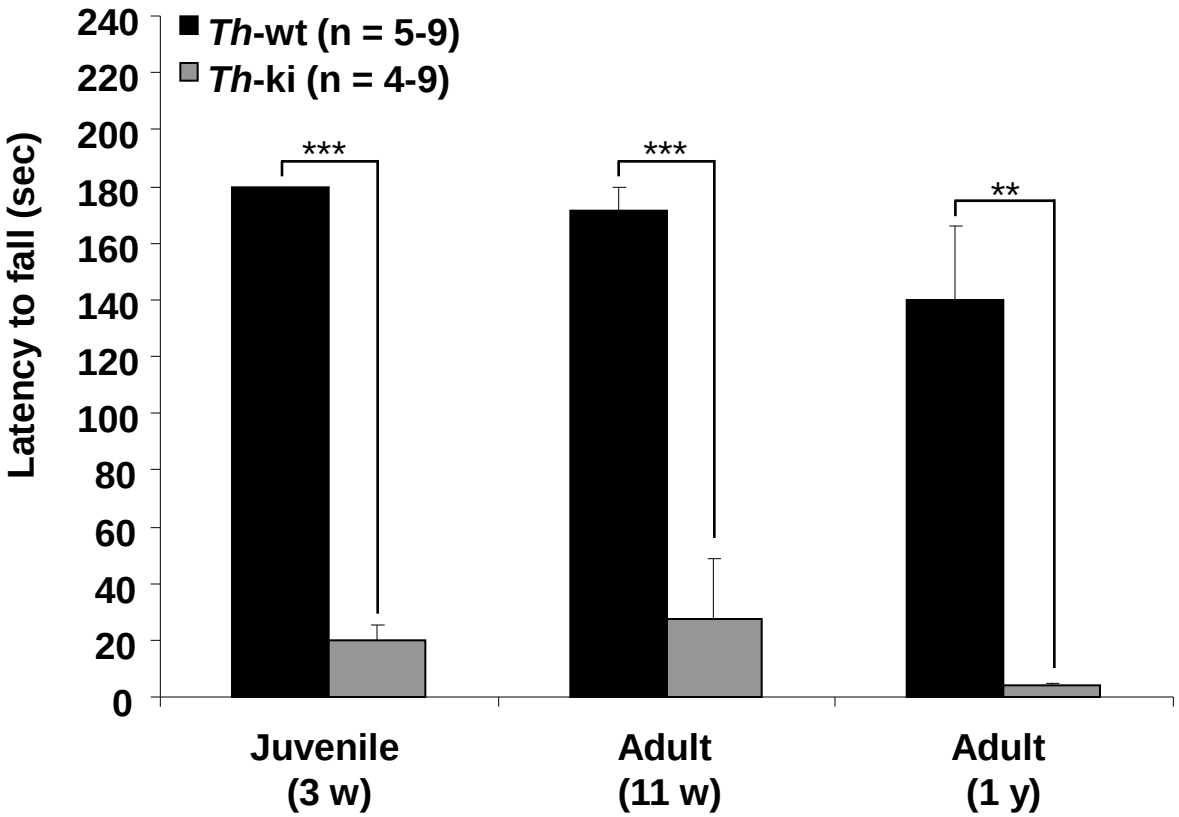

Fig. 3B, Korner et al

C **Open field test: distance**

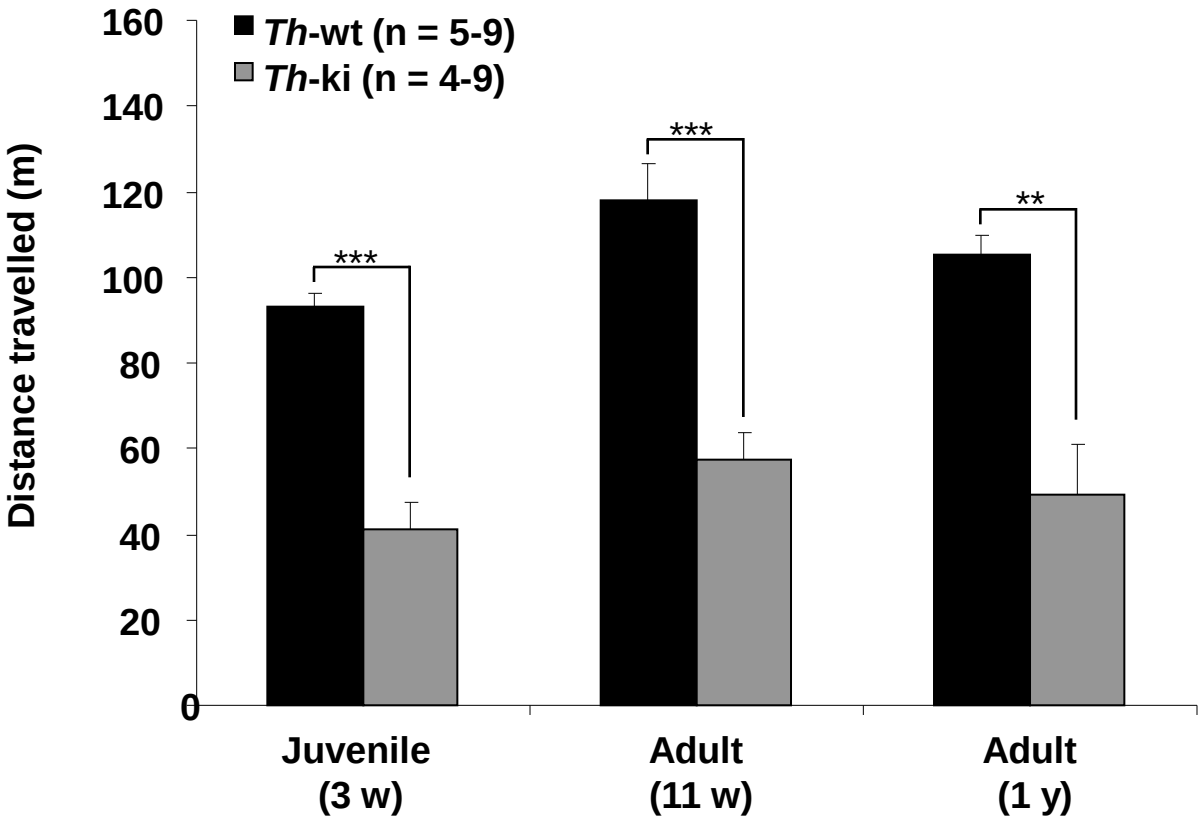

Fig. 3C, Korner et al

D Open field test: velocity

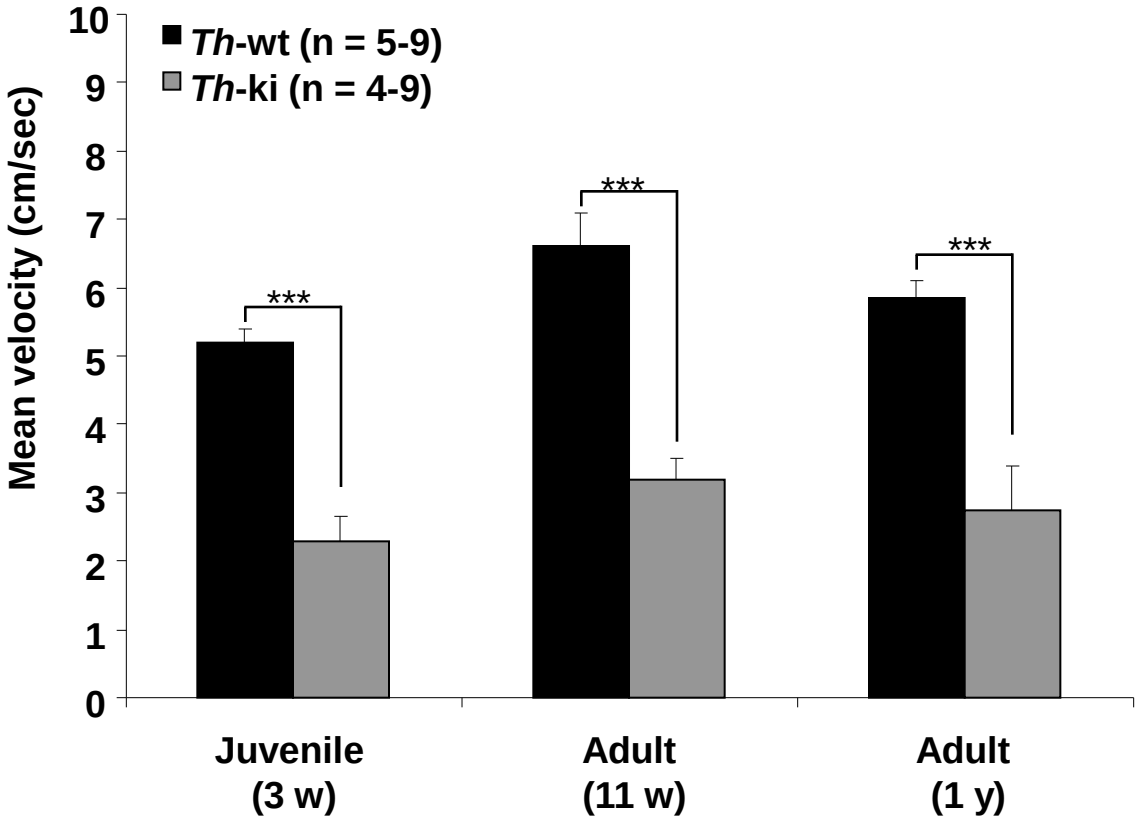

Fig. 3D, Korner et al

E **Gait analysis: wide-based gait**

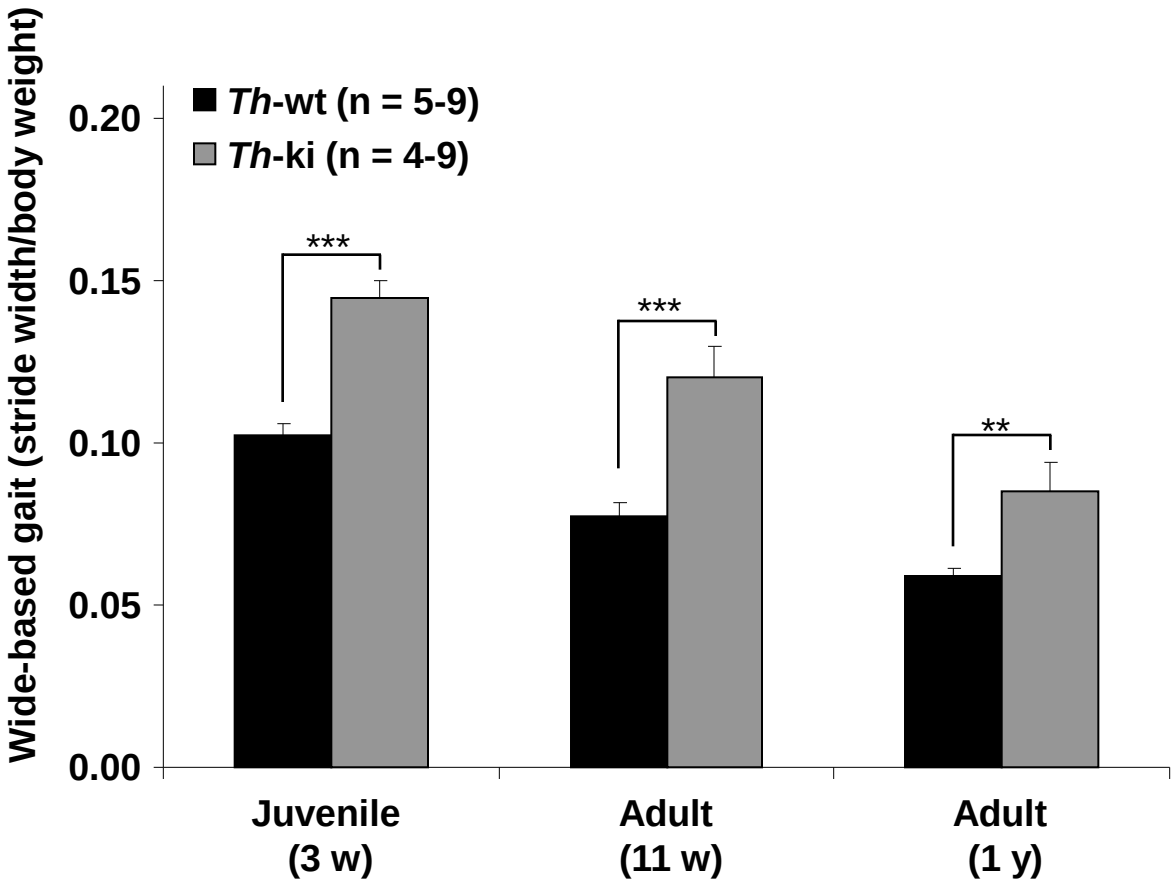

Fig. 3E, Korner et al

F **Gait analysis: short-step**

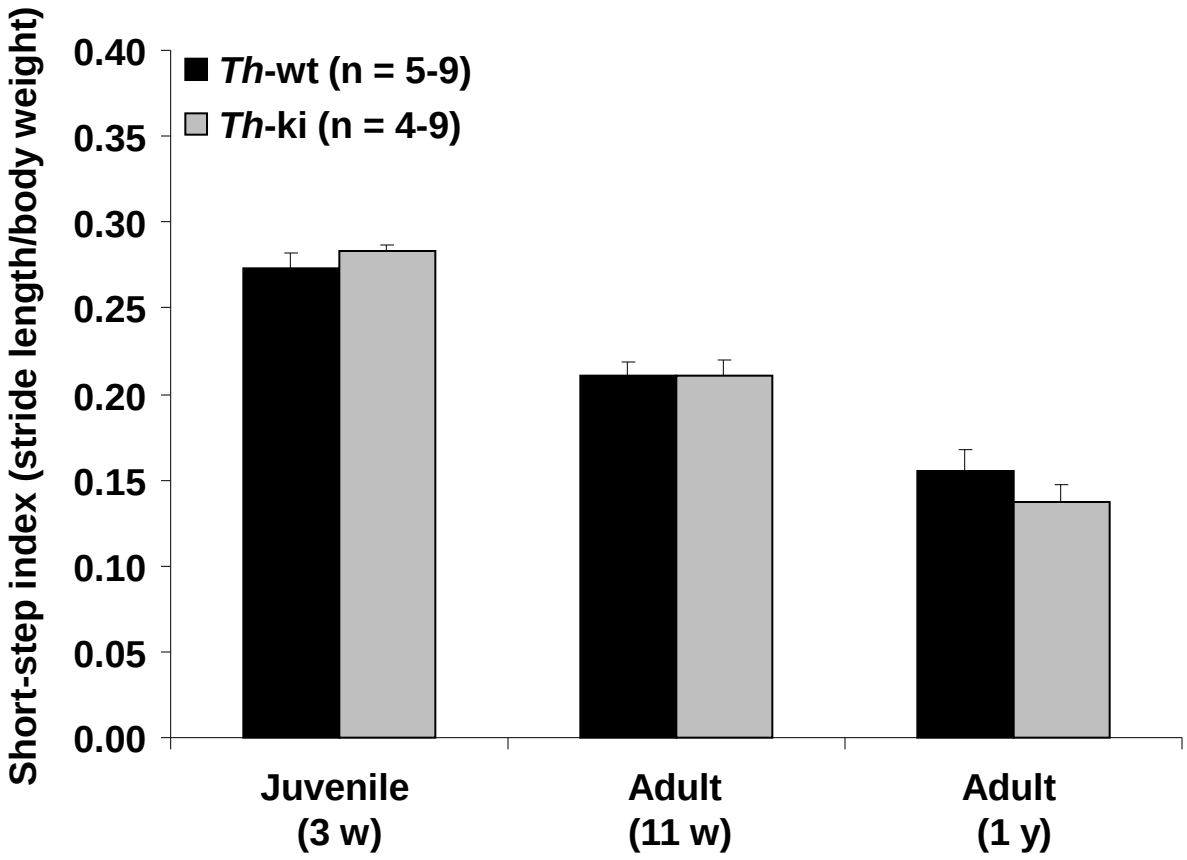

Fig. 3F, Korner et al

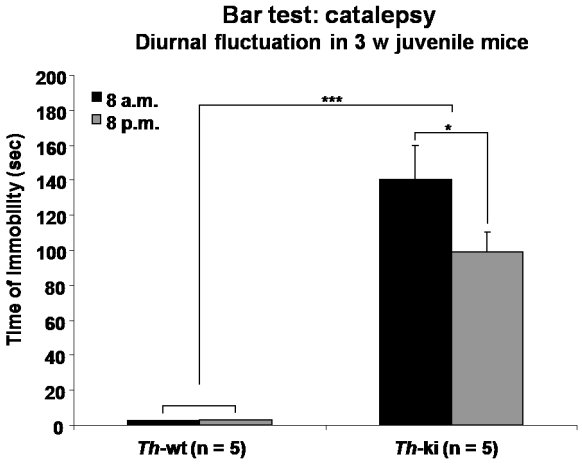

Fig. 4, Korner et al

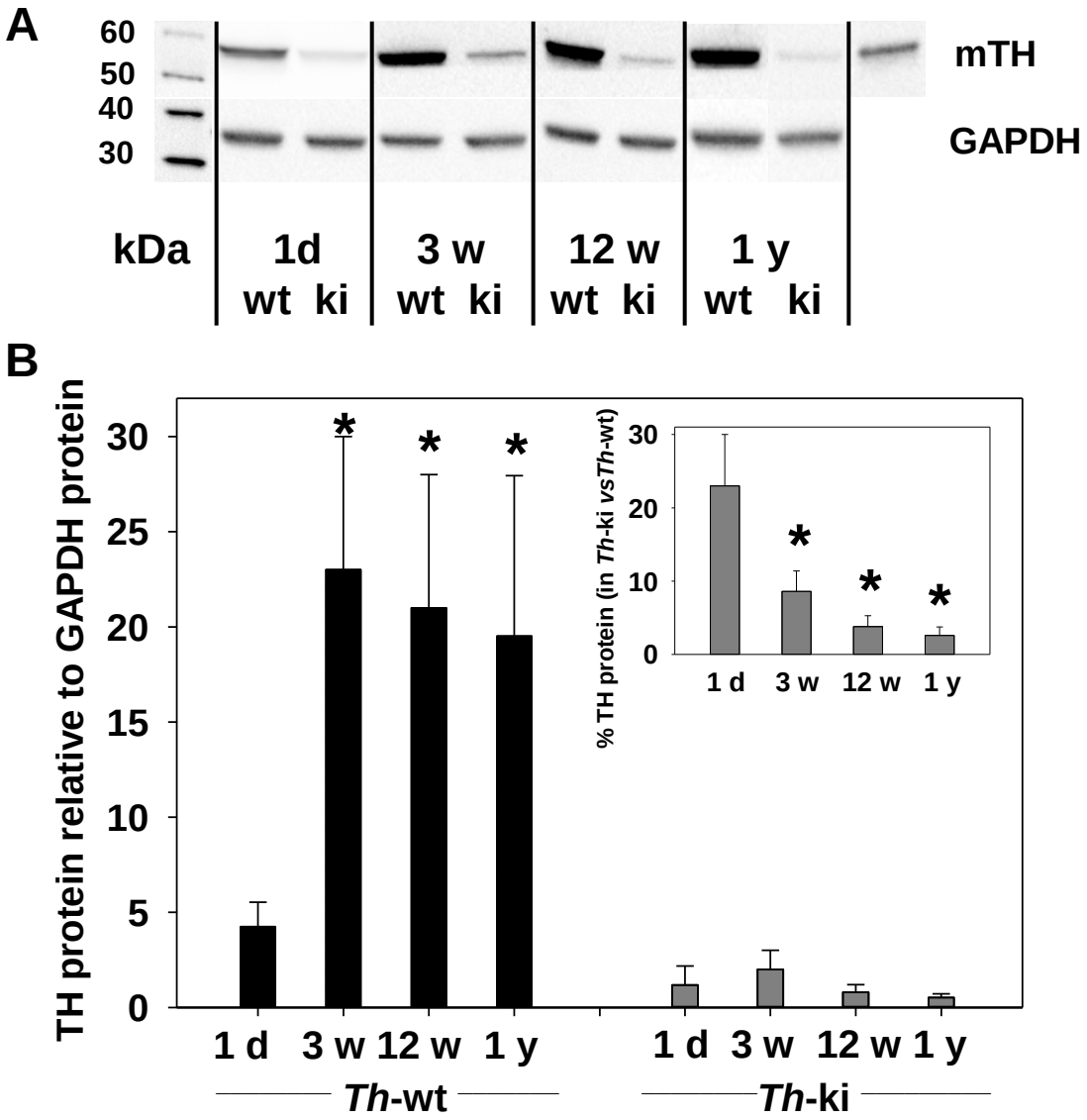

Fig. 5A-B, Korner et al

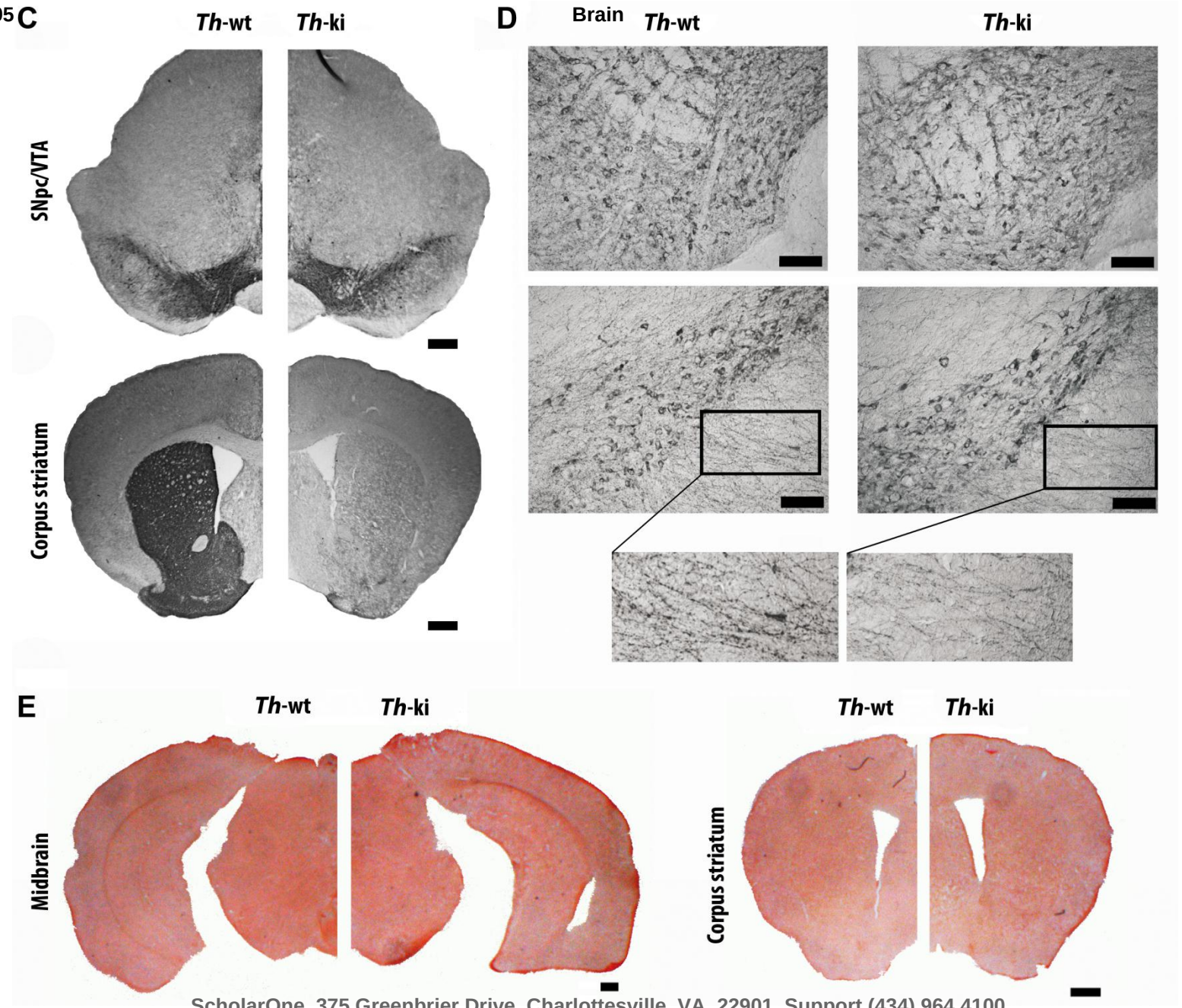

Fig. 5C-E, Korner et al

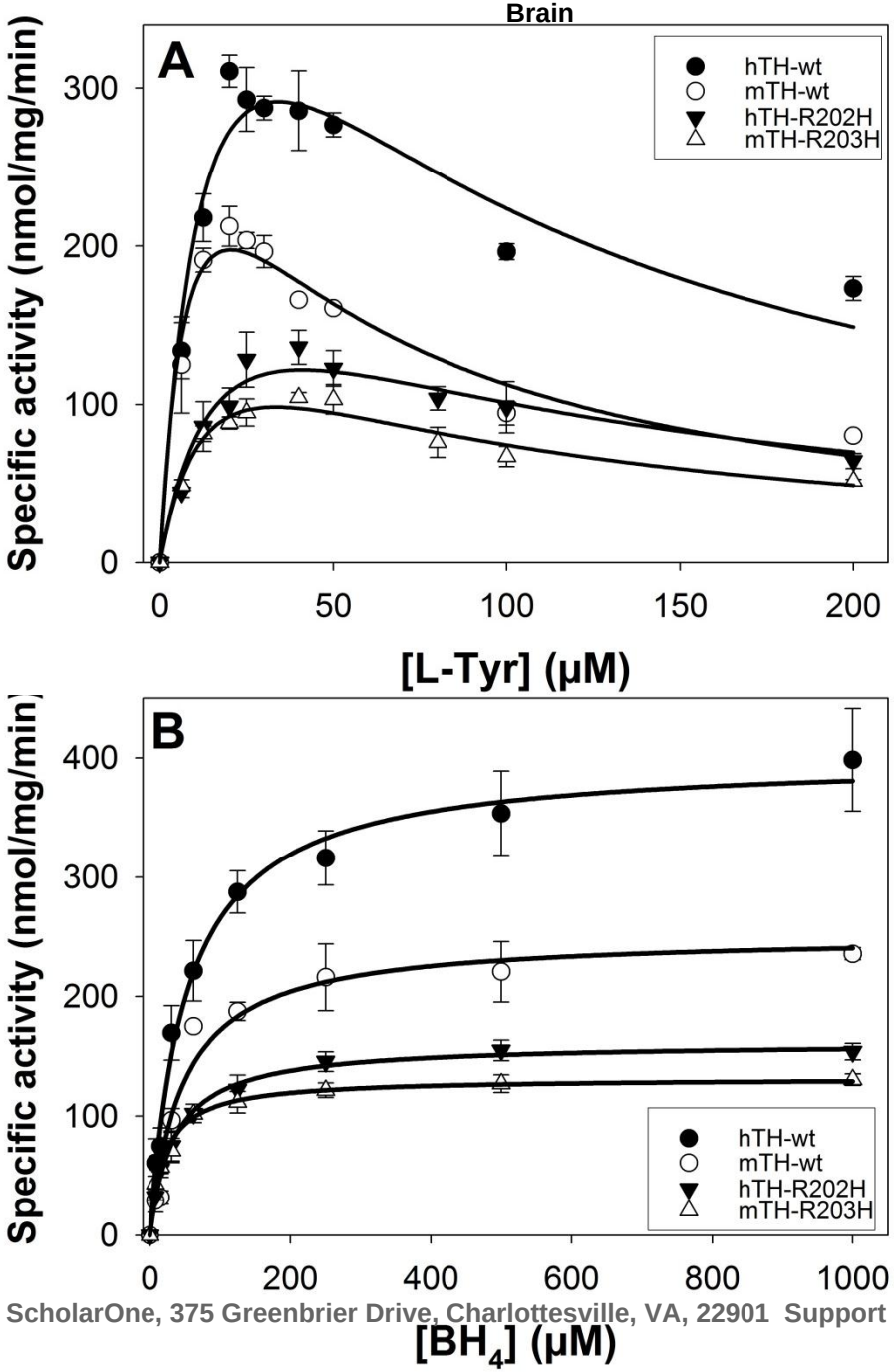

Fig. 6A-B, Korner et al

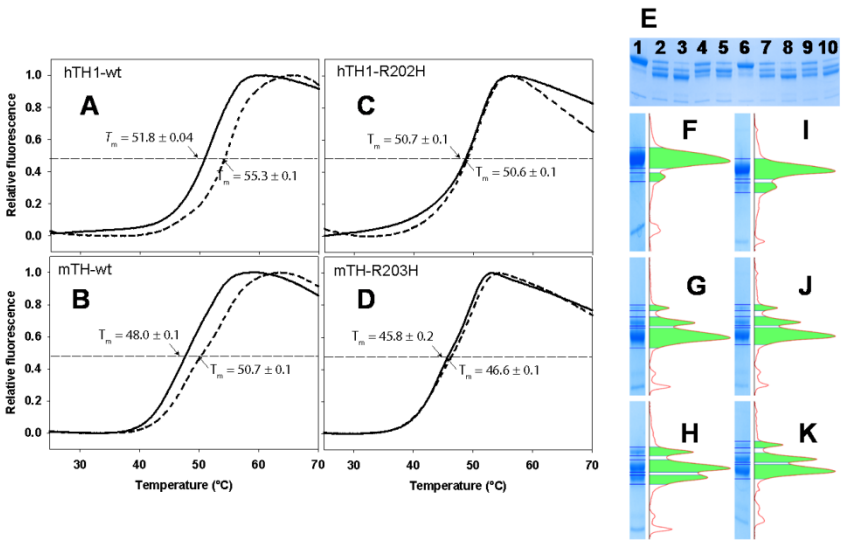

Fig. 7A-K, Korner et al

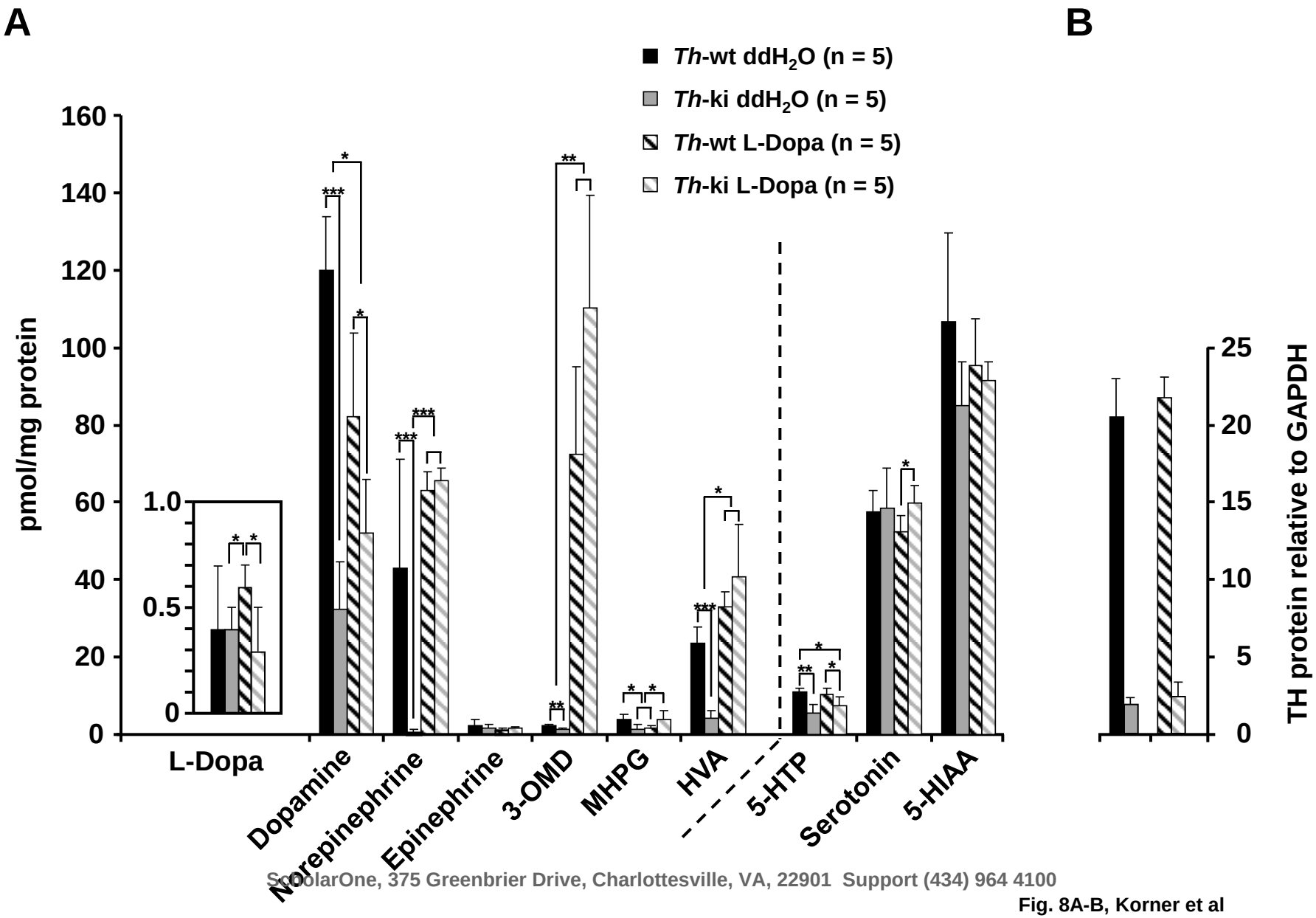

Fig. 8A-B, Korner et al

Supplementary Methods

Analytical methods for in vitro and in vivo characterization of (human) hTH1 and (mouse) mTH wt and mutant enzymes

***Cloning of mouse mTh into pET-MBP-1a*:** The pSL1180 vector containing mouse *Th* (m*Th*) cDNA was a generous gift from Prof. Hiro Ichinose (Tokyo Institute of Technology, Japan) and used as template DNA in a PCR with the following primers: 5'-GCTTCCATGgga CCCACCCCCAG-3' and 5'-GCTTGGTACCTTAGCTAATGGCA-3'. This amplifies the m*Th* gene with an *Nde*I site in the 5' end and an *Acc*65I site after the stop codon. Restriction sites in the primers are underlined and lowercase letters indicate bases inserted to facilitate restriction (translates into an extra glycine in position 2). The m*Th* PCR-products and pET-MBP-1a/h*TH*1 (the cloning of h*TH*1 into the pET-MBP-1a vector will be published elsewhere (Bezem et al., to be submitted)) were cut with NcoI and Acc65I and purified before mixed in a ligation reaction to produce pET-MBP-1a/m*Th*. The correct pDNA was detected by colony PCR and verified by sequencing.

***Mutagenesis of human and mouse TH and expression and purification of the recombinant proteins*:** The mutagenic primers 5'-CAGGTGTACCGCCAGCACAGG AAGCTGATTGCTGAG-3' and 5'-GCGTATCGCCAGCATCGGAAGCTGATTGC-3' (and their complements) were used to generate the pET-MBP-1a/h*TH*1-R202H and pET-MBP-1a/m*Th*-R203H mutants, respectively, using QuikChange mutagenesis (Stratagene). The mutated bases are underlined. Correct mutations were verified by sequencing. hTH1-wt, mTH-wt, hTH1-R202H and mTH-R203H were expressed as His-MBP-TH fusion proteins in *E. coli* strain BL21 using LB medium with induction by 1 mM IPTG, isolated on amylose resin and eluted with 10 mM maltose. Fusion proteins were cut for 1 hour at 4 °C using TEV-protease at a TH:TEV ratio of 10:1. Tetrameric TH-proteins were isolated using size-exclusion chromatography on a HiLoad Superdex200 column (GE Healthcare), leaving the protein in 20 mM NaHepes pH 7, 200 mM NaCl. The proteins were homogeneous and contained correct N-terminal sequence (as seen by MS-spectroscopy; not shown).

***Immunodetection*:** Brain extracts (prepared as described above) were clarified by centrifugation at 20,000g for 15 min at 4°C. Free amino acids and contaminants of low molecular weight were removed from the supernatants using Zeba desalting spin columns (Thermo Scientific), and then the supernatants were stored in liquid nitrogen prior to use. Protein concentration was measured with Direct Detect (Merck Millipore). Quantification of TH protein was performed by western blot analyses after SDS-PAGE (10% acrylamide) with 20 µg total protein in each lane, and transfer to nitrocellulose membrane and immunostaining using affinity-purified polyclonal rabbit anti-rat TH (Thermo Scientific) in a 1:1,000 dilution as primary antibody. Secondary antibody was goat anti-rabbit IgG horseradish peroxidase conjugate (Bio-Rad) in a 1:2,000 dilution. The membrane was also immunostained with a polyclonal antibody against GAPDH (Abcam) as a loading control. Purified recombinant

hTH1 (10 ng/lane) was used as standard for immunoquantification. Detection was performed by enhanced chemiluminescence (ECL; Amersham), and immunoquantification in a Molecular Image using Image Lab 3.0.1 software (Bio-Rad).

***Tyrosine hydroxylase activity assay*:** TH activity in brain extracts was assayed at 30°C immediately following the preparation of the extracts (see above) as described (Reinhard *et al.*, 1986), with the modifications reported (Thöny *et al.*, 2008), using an incubation mixture containing 100 mM NaHepes, pH 7.0, 50 µM L-[3,5-^{3}H]-tyrosine, 0.05 mg/ml catalyse, 20 µM ferrous ammonium sulphate, and 100 µM 3-hydroxybenzyl hydrazine (NSD-1015, an inhibitor of L-aromatic amino acid decarboxylase). The enzyme was pre-incubated for 1 min in this mixture, and the reaction started by addition of 500 µM BH_4 and 5 mM DTT. The reaction was stopped after 30 min by addition of 1 ml of 7.5% activated charcoal suspension in 1 M HCl. After centrifugation at 10,000 g, the supernatant was counted in a scintillation counter. TH activity of the purified TH enzymes was assayed at 25 °C, essentially as described (Haavik and Flatmark, 1980), with certain modifications. The incubation mixture contained 40 mM NaHepes, pH 7.0, 0.1 mg/ml catalase, 10 µM ferrous ammonium sulphate and 25 µM L-Tyr. To this0 mixture the enzyme was added to a final concentration in the assay of 0.01 mg/ml (0.16 µM subunit, diluted in 0.1 mg/ml bovine serum albumin and 2 µM ferrous ammonium sulphate, in 20 mM NaHepes, pH 7.0, 200 mM NaCl). The reaction was started by adding 200 µM BH_4 (Schircks Laboratories) with 2 mM DTT, and stopped after 5 min, by adding an equal volume of 2% (v/v) acetic acid in ethanol. After precipitation of the enzyme, L-Dopa was separated and measured by HPLC with fluorimetric detection ((λ_{ex} = 274 nm, λ_{em} = 314 nm). The L-Tyr-concentration dependence was analyzed in the range 6.25 to 100 µM at a fixed concentration of BH_4 of 200 µM and 2 mM DTT. The BH_4-concentration dependence was analyzed in the range 16 to 1000 µM (and fixed DTT and L-Tyr concentrations of 2 mM and 25 µM, respectively). The results were analyzed using the enzyme kinetics function in SigmaPlot, where the K_m and V_{max} values, in the case of BH_4-dependency and the $S_{0.5}$(L-Tyr) and K_{si} for the substrate inhibition by L-Tyr were obtained using Michaelis-Menten and substrate-inhibition equations, respectively.

***Differential scanning fluorimetry (DSF)*:** DSF was used to measure the thermal stability of purified hTH1, mTH, hTH1-R202H and mTH-R203H, with and without DA. 0.9 µM hTH1 (subunit concentration) was incubated with 3X ferrous ammonium sulphate and 5X Sypro Orange before added to DA-containing wells of a 96 well-plate. A LightCycler 480 Real-Time PCR System (Roche Applied Science) was used to heat the plate from 25°C to 90°C at a heating rate of 2°C/min. Thermal denaturation of TH was monitored by detecting the increase in Sypro Orange fluorescence (λ_{ex} = 465 nm, λ_{em} = 610 nm) upon its binding to exposed hydrophobic patches. The data was scaled to reflect fraction unfolded and midpoint denaturation (T_m). T_m-values were determined as maximal temperature in a first-derivative plot.

***Limited proteolysis by trypsin*:** The susceptibility of TH to limited proteolysis by trypsin was performed at 25 °C, as described (Flatmark *et al.*, 1999), with some modifications. hTH1 or hTH1-R202H (0.14 mg/ml) was incubated with TPCK-treated trypsin (Sigma) at a TH:trypsin ratio of 200:1 in 20 mM NaHepes, pH 7.4, 200 mM NaCl, in presence or absence of 50 µM DA. Trypsin soybean inhibitor (1.5 µg/ml; Sigma) and SDS-buffer were added to stop the reaction and perform SDS-PAGE (10 %) at 180 V. The gels were stained with Coomassie Brilliant Blue and scanned using ChemiDoc XRS+ from BioRad. The raw volume of the bands was measured using the Image Lab 3.0.1 software. The amino acid sequence of the protein bands was obtained in the excised bands after reduction, alkylation and in-gel trypsinization and LC (liquid chromatography)–MS/MS (tandem MS) analysis following standard procedure (Shevchenko *et al.*, 2006, Berle *et al.*, 2013) The MS and MS/MS raw data files were processed using Proteome Discoverer 1.4 software.

Supplementary Table S1: Gene (*mRNA*) expression of *Th* and *Tph*1/2 in brain of mice at different ages

Genotype	Age	*Th*-mRNA[a]	*Tph*1-mRNA[a]	*Tph*2-mRNA[a]
Th-wt newborn (n = 4)	1 day	1.00 (0.65 - 1.55)	0.09 (0.03 - 0.23)	0.06 (0.01 - 0.31)
Th-ki newborn (n = 4)	1 day	1.06 (0.74 - 1.53)	0.06 (0.06 - 0.07)	0.08 (0.03 - 0.26)
Th-wt juvenile (n = 5)	3 weeks	1.48 (0.71 - 3.10)	0.03 (0.02 - 0.03)	0.14 (0.03 - 0.61)
Th-ki juvenile (n = 5)	3 weeks	1.62 (1.31 - 2.01)	0.03 (0.02 - 0.05)	0.07 (0.03 - 0.20)
Th-wt adult (n = 5)	12 weeks	1.46 (0.94 - 2.27)	0.04 (0.03 - 0.04)	0.05 (0.02 - 0.10)
Th-ki adult (n = 5)	12 weeks	1.96 (1.23 - 3.41)	0.03 (0.02 - 0.05)	0.03 (0.01 - 0.06)
Th-wt adult (n = 4)	1 year	1.60 (0.84 - 3.03)	0.04 (0.02 - 0.07)	0.03 (0.01 - 0.06)
Th-ki adult (n = 4)	1 year	1.46 (0.89 - 2.42)	0.04 (0.02 - 0.05)	0.01 (0.00 - 0.04)

[a] Normalized relative to *Gapdh*-mRNA (Livak and Schnittgen, *Methods 25*(4):402-408, 2001)
Th tyrosine hydroxylase; *Tph*1/2 tryptophan hydroxylases 1 and 2; *Gapdh*, glyceraldehyde 3-phosphate dehydrogenase

Supplementary Table S2: Ratio of HVA : 5-HIAA in brain homogenates from *Th*-ki mutant and *Th*-wt mice

Age of Mice	*Th*-ki	*Th*-wt	Average Reduction in Th-*ki* mice (%)
Newborn (1 day; n = 5)	0.016 (0.008 - 0.020)	0.039 (0.027 - 0.050)	60
Juvenile (3 weeks; n = 5)	0.104 (0.063 - 0.135)	0.294 (0.256 - 0.394)	65
Adults (12 weeks; n = 5)	0.030 (0.014 - 0.044)	0.343 (0.234 - 0.502)	91
Adults (1 year; n = 5)	0.054 (0.018 - 0.144)	0.237 (0.143 - 0.313)	77

A

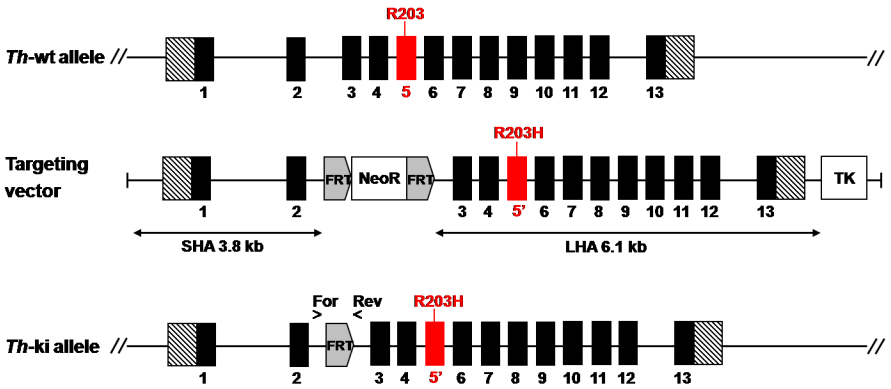

Supplementary Fig. S1A,
Korner et al

B

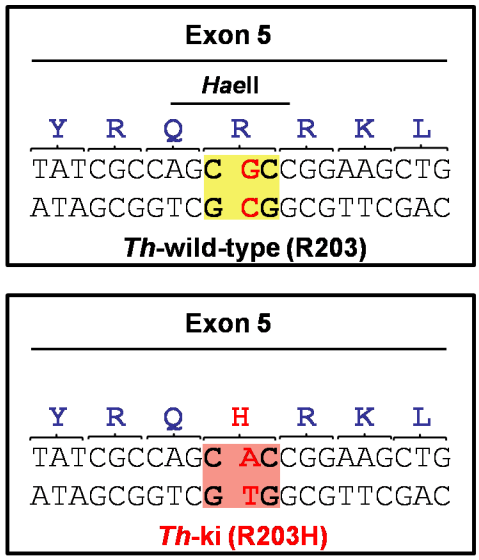

Supplementary Fig. S1B,
Korner et al

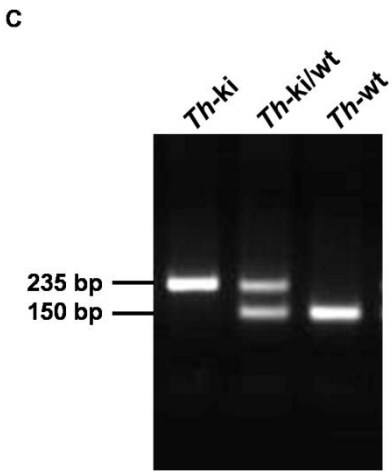

Supplementary Fig. S1C,
Korner et al

A

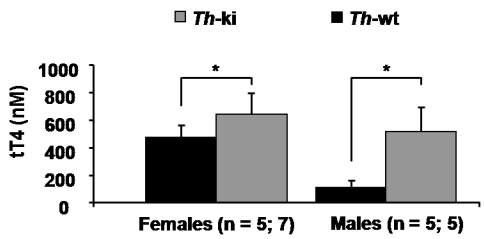

Supplementary Fig. S3A, Körner et al

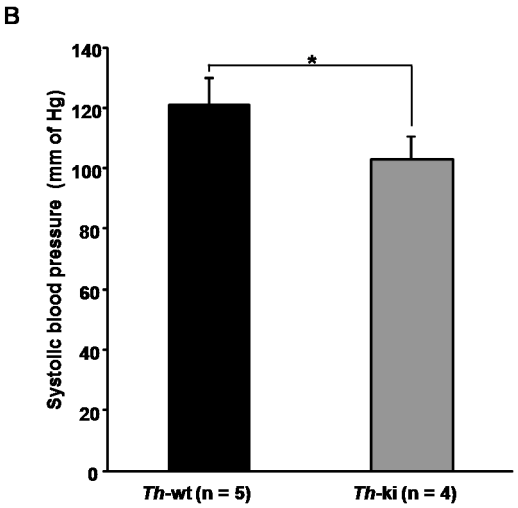

Supplementary Fig. S3B, Körner et al

C

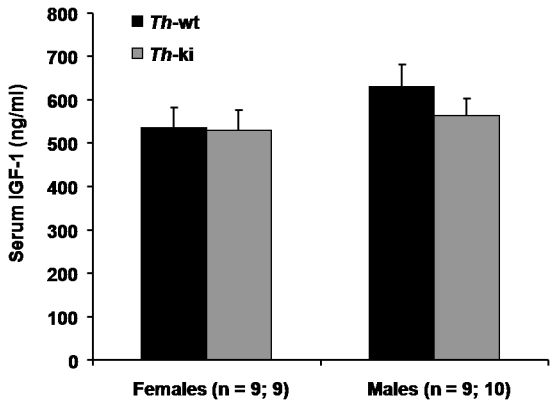

Supplementary Fig. S3C, Korner et al

D

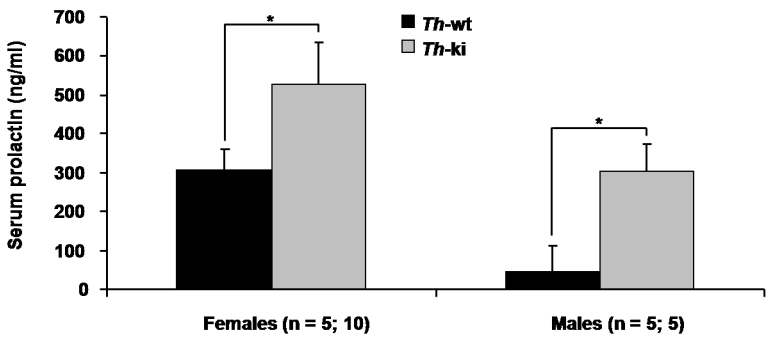

Supplementary Fig. S3D, Körner et al

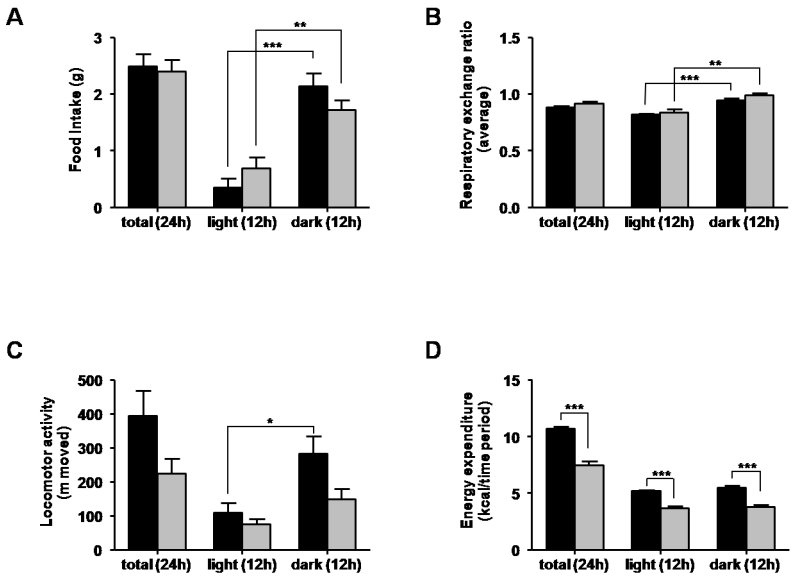

Supplementary Fig. S2A-D, Körner et al

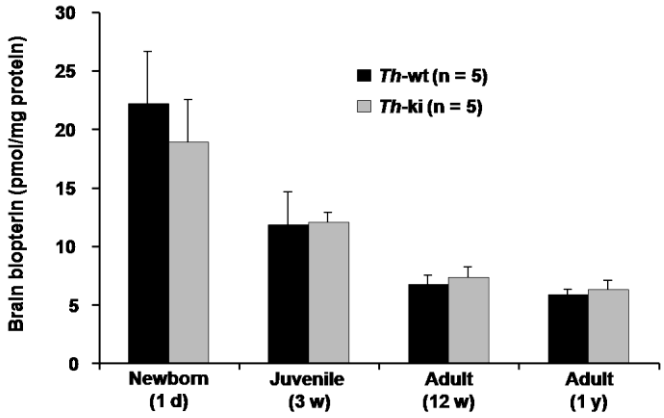

Supplementary Fig. S4, Korner et al

A Bar test: Newborn mice treated for 3 weeks with L-Dopa

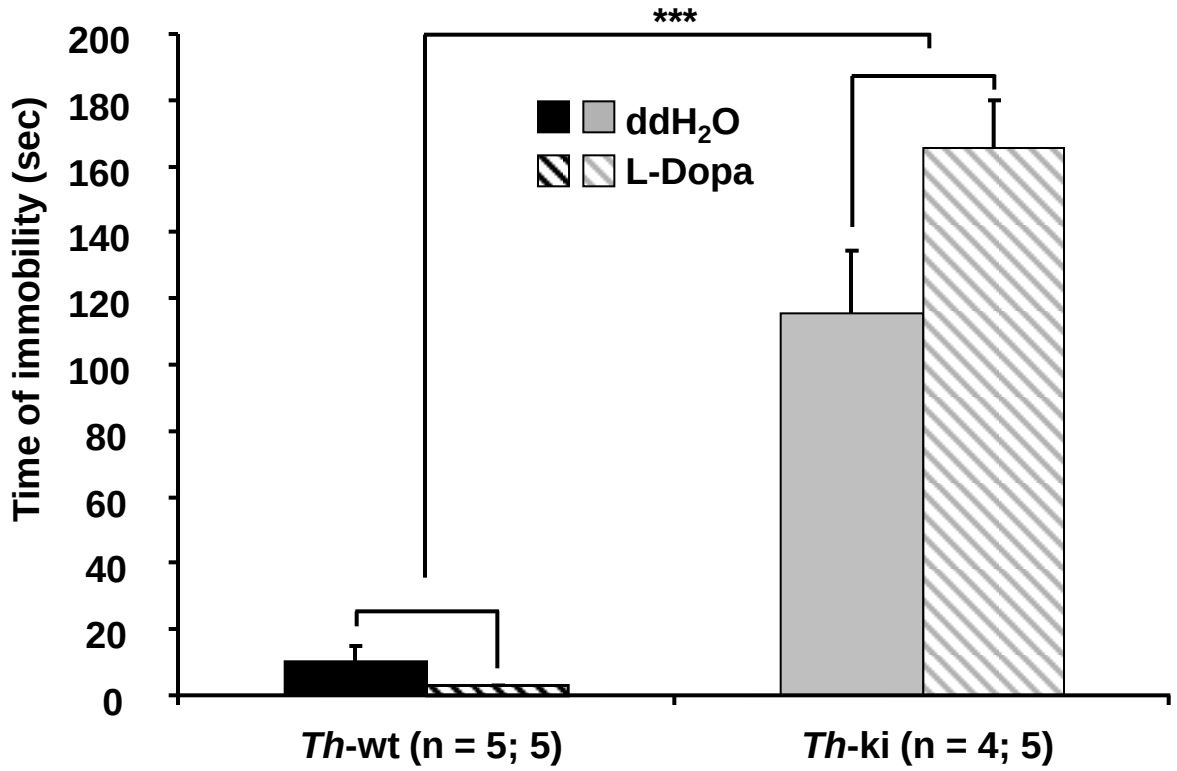

Supplementary Fig. S5A, Korner et al

B Rotarod test: Newborn mice treated for 3 weeks with L-Dopa

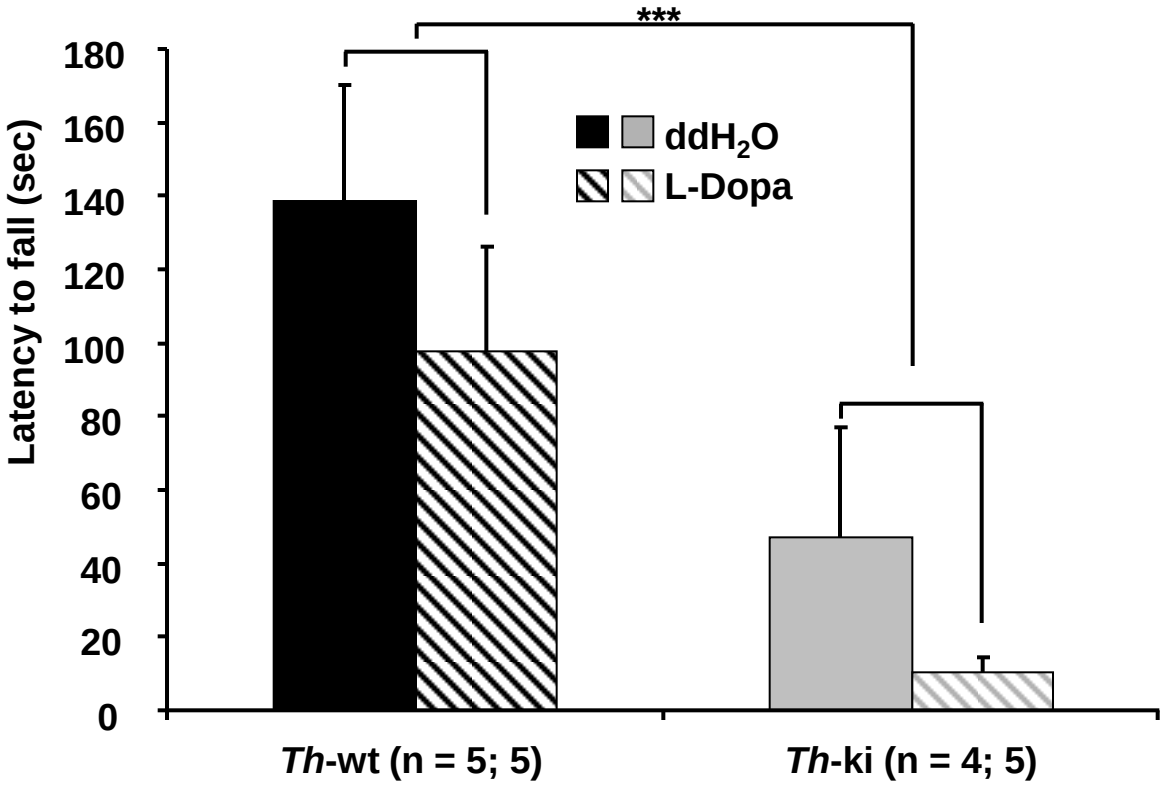

Supplementary Fig. S5B, Korner et al

C Bar test: Acute treatment of adult mice with L-Dopa

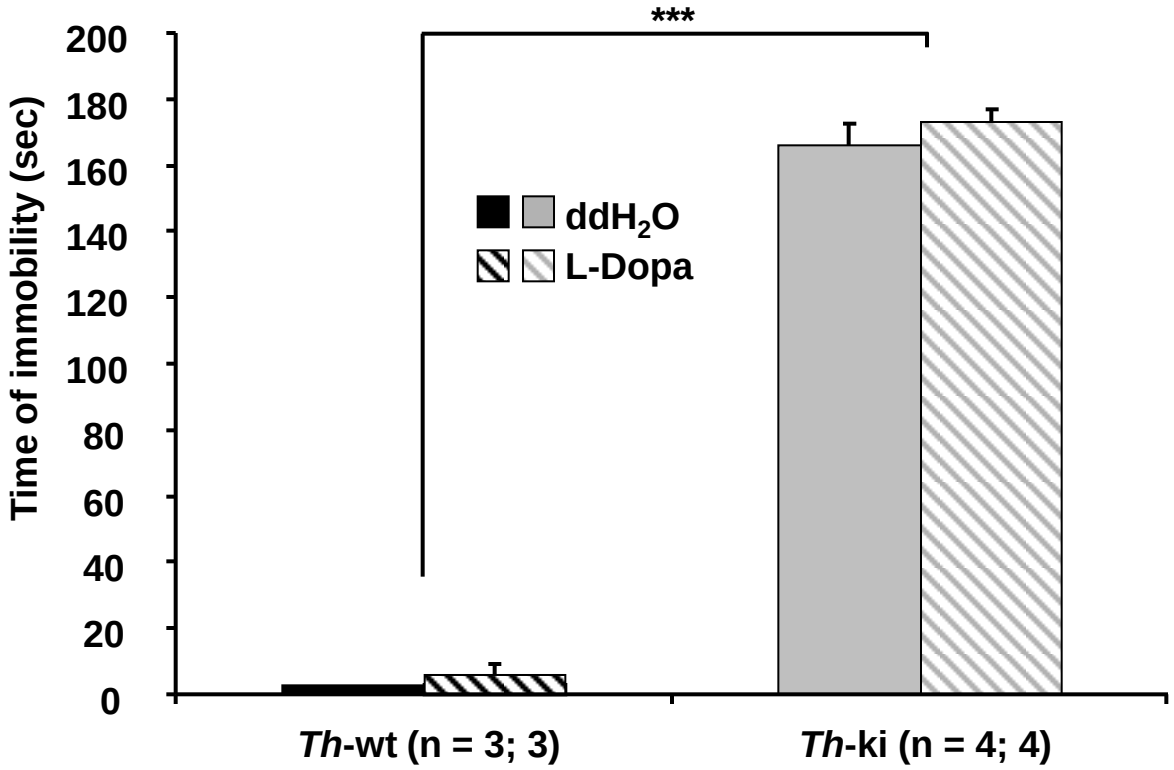

Supplementary Fig. S5C, Korner et al

D Rotarod test: Acute treatment of adult mice with L-Dopa

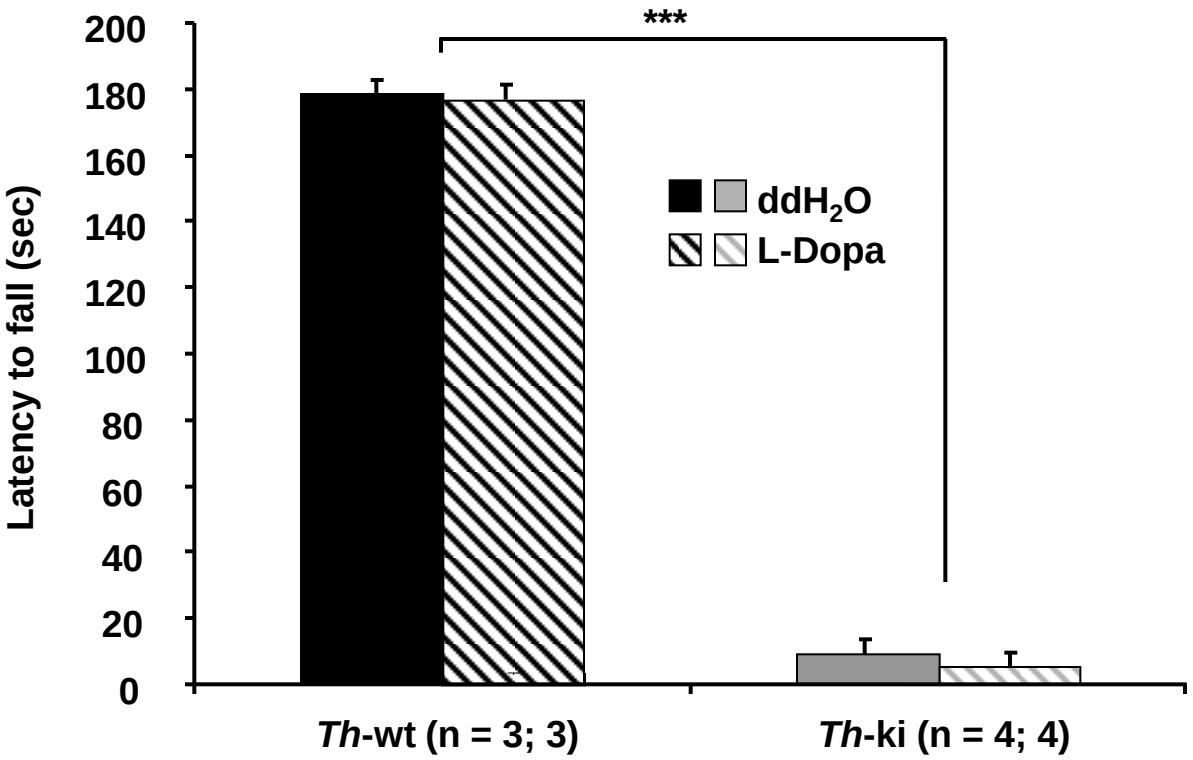

Supplementary Fig. S5D, Korner et al